

UC Berkeley

UC Berkeley Electronic Theses and Dissertations

Title

STUDYING MEMBRANE ANCHOR ORGANIZATION IN LIVING CELL MEMBRANES

Permalink

<https://escholarship.org/uc/item/7z73k11z>

Author

Huang, Hector Han-Li

Publication Date

2011

Peer reviewed|Thesis/dissertation

STUDYING MEMBRANE ANCHOR ORGANIZATION IN LIVING CELL MEMBRANES

by

Hector H. Huang

A dissertation submitted in partial satisfaction of the

requirements for the degree of

Doctor of Philosophy

in

Molecular & Cellular Biology

in the

Graduate Division

of the

University of California, Berkeley

Committee in charge:

Professor Jay T. Groves, Co-chair

Professor Eva Nogales, Co-chair

Professor Susan Marqusee

Professor Dan Fletcher

Spring 2011

ABSTRACT

STUDYING MEMBRANE ANCHOR ORGANIZATION IN LIVING CELL MEMBRANES

by

Hector Han-Li Huang

Doctor of Philosophy in Molecular and Cell Biology

University of California, Berkeley

Professor Jay T. Groves, Co-chair

Professor Eva Nogales, Co-chair

The cell membrane is a complex mixture of various lipids, proteins and other biomolecules that are all organized into a fluid 2-dimensional bilayer. A rather unique trait of this organelle is the lateral mobility of the component molecules. Surprisingly, these molecules are not necessarily distributed homogeneously in the membrane. From a physical perspective, these inhomogeneities are interesting because they indicate some level of organization in the membrane. From a biological perspective, this organization is interesting because it might be a key regulatory element in the enzymatic processes and cell signaling events that occur at the cell membrane. Due to the difficulty of studying membrane organization, not much is known about the spatiotemporal scale of these organized domains, nor is it clear what the physical driving forces are, although there are models based on observations from a variety of different methods. The key factor to overcome in studying membrane organization is the ability to probe the membrane in an informative way that does not perturb the native organization of the membrane.

Membrane anchors are lipid moieties covalently conjugated to various membrane proteins and have been implicated in the lateral sorting of anchored proteins in the membrane. Most studies on lipid anchors focus either on identifying what molecules anchored proteins colocalize with or observing how anchored proteins diffuse in the cell membrane. Truncated anchored proteins with just the anchor domain remaining can be genetically fused to fluorescent proteins and also studied to determine the extent to which the anchor-membrane interactions, as opposed to protein-protein interactions, influence their distribution in the membrane. The methods used to study these behaviors are varied and, subsequently, the observations that result from these studies are also varied and the conclusions are conflicting.

Time-resolved spectroscopy of fluorescently labeled anchor domains in living cells offers a non-invasive method to extract a wealth of information about the spatiotemporal localization of anchored proteins in a live cell. More specifically, fluorescence cross-correlation spectroscopy (FCCS) analysis and fluorescence lifetime analysis can be derived from the same data stream. In this dissertation, I review the current model of how membranes are organized and present observations made by myself and coworkers, of two instances of homogeneous colocalization of the same anchors but no heterogeneous colocalization of different anchors in Jurkat cell membranes. We conclude that the observation of two distinct non-overlapping domains existing in the same cell membrane indicate a more complex organization than the current model allows.

I dedicate this work to my family and friends for all their love and support.

Table of Contents

List of Figures	iv
List of Equations	v
Acknowledgements	vi
1 Introduction	1
1.1 Abstract	2
1.2 Lateral inhomogeneities in the plasma membrane	2
1.3 Membrane Anchors	2
1.3.1 Membrane anchored proteins may be organized in the membrane	3
1.3.2 GPI anchors exhibit specific localization	3
1.3.3 N-myristoylation and S-acylation are believed to promote colocalization	3
1.3.4 Isoprenyl groups are unsaturated.....	4
1.3.5 Lipid anchors are markers for membrane organization.....	4
1.4 Lipid Raft Model	5
1.4.1 Lipid rafts mean different things	5
1.4.2 Lipid rafts were first thought of as DRMs.....	6
1.4.3 Model Membrane Phase Separation.....	6
1.4.4 Phase separated vesicles do not represent domains in membranes	7
1.4.5 Better resolution of smaller features.....	8
1.4.6 Diffusional studies.....	9
1.4.7 Picket Fence Model	9
1.4.8 Does the raft model predict sorting?	10
2 Specific Lipid-Anchor Organization in Cell Membranes is Revealed by PIE-FCCS	11
2.1 Abstract	12
2.2 Introduction	12
2.3 Materials and Methods	14
2.3.1 Cloning	14
2.3.2 Protein Expression and Purification	14
2.3.3 Supported Lipid Bilayer Formation and Protein binding	14
2.3.4 Cell Culture/Transfection/Sample preparation.....	15
2.3.5 PIE-FCCS	16

2.3.6 Lifetime acquisition.....	16
2.3.7 Data Analysis.....	17
2.4 Results	17
2.4.1 Live cells express lipid anchored fluorescent proteins.....	17
2.4.2 Relative correlation is measured by PIE-FCCS	18
2.4.3 Relative correlation is dependent on density	21
2.4.4 Relative correlation is anchor specific	21
2.4.5 Relative correlation is cell-specific	22
2.4.6 Fluorescence lifetimes show no energy transfer	23
2.5 Discussion	23
2.6 Acknowledgements	26
2.7 Supporting Information	27
3 Practical considerations for PIE-FCCS of lipid anchors in live cells.....	29
3.1 Abstract	30
3.2 Expression Level	30
3.2.1 Density Range	30
3.2.2 Different Expression Systems	30
3.3 Cell type	31
3.3.1 Different cell types have different membranes	31
3.3.2 Notes on sample preparation	32
3.4 Empirical states of Correlation.....	32
3.4.1 Cross-correlation values should be mapped to known physical states.....	32
3.4.2 Protein “freshness” is critical in <i>in vitro</i> experiments	33
3.5 FCCS	33
3.5.1 FCS/FCCS is used to study a number of dynamic processes.....	33
3.5.2 Choosing the right fluorophores.....	34
3.5.3 Power Scan	34
3.5.4 Spot Size Measurement	35
3.5.5 TCSPC advantage and disadvantage	36
3.5.6 Spot selection in cells	37
Bibliography	38
Appendix A	42

List of Figures

Figure 1.1 Membrane anchors are mainly composed of some lipid moieties and charged residues.	5
Figure 1.2. Cartoon depicting classical model of lipid raft.	7
Figure 2.1. Epifluorescence of Jurkat cells expressing anchored fluorescent proteins shows homogeneous distribution in the plasma membrane.	17
Figure 2.2. PIE-FCCS acquisition generates cross-talk free data.	18
Figure 2.3. Empirical Mapping of Correlated States.	20
Figure 2.4. Comparison of relative cross-correlation of different membrane anchors in Jurkat cells.	22
Figure 2.5. Fluorescence lifetimes do not show evidence of energy transfer.	23
Figure 2.6. Physical Model of anchor clustering.	24
SI Figure 1. Epifluorescence of Jurkat cells expressing K-Ras anchor fluorescent fusion protein shows homogeneous distribution in the plasma membrane.	27
SI Figure 2. Epifluorescence of COS 7 cells and comparison of relative cross-correlation of different membrane anchors in COS 7 cells.	28
Figure 3.1. HEK 293T and MDCK cells expressing anchored fluorescent proteins.	32
Figure 3.2. Example of good and bad bilayers	33
Figure 3.3. Power scan of GFP and Cherry.	35
Figure 3.4. TCSPC card dead time decreases cross-correlation.	36

List of Equations

Equation 2.1 Autocorrelation Function.	19
Equation 2.2 Cross-correlation Function.	19
Equation 2.3 F_{cross} defined.	19
Equation 2.4 2D diffusional model.	21
Equation 2.5 Poisson probability of probes per cluster.	25
Equation 2.6 Scaled Poisson probability of other probes per cluster.	25
Equation 2.7 Normalized Poisson probability.	25
Equation 2.8 Binomial probability of cross-correlation.	25
Equation 2.9 Total probability of cross-correlation.	25
Equation 3.1 τ_D defined.	35

Acknowledgements

I would like to thank everyone who has helped me with this work. I would like to thank Professor Jay Groves for his support over the last six years, for his patience with my progress, and for teaching me how to conduct and communicate science. I would like to especially thank Sara Triffo for being a gracious and thoughtful collaborator. I owe my success to your efforts. Eldon deserves a great deal of my thanks, for being the first and only undergraduate student I have mentored. You've been a great resource and you have taught me to verbalize difficult ideas. I would like to thank Dr. Adam Smith for also being a helpful collaborator on this project. I would like to thank all the members of the Groves lab, for years of engaging discussion, encouraging help, and enlightening entertainment, but I would especially like to thank select members for their help with this project. Thanks to Il-Hyung Lee and Mike Coyle for a lot of very useful discussion about FCS and FCCS and for sharing your resources with me. Thanks to Dr. Wan-Chen Lin for all your patience in teaching me about the instrument and for many hours of useful discussion. Thanks to Alex Smoligovets for help with cell culture resources and for useful advice about different cell types. Thanks to Dr. Niña Hartman for managing the lab and to Dr. Pradeep Nair for (too) many hours of discussion.

Thanks to Professor Björn Lillemeier and Professor Mark Davis for the original membrane anchor constructs and to Dr. Nick Endres and Professor John Kuriyan for the K-Ras constructs. Thanks to Dr. Ann Fischer for all tissue culture cell lines and a great deal of tissue culture help.

A lot of thanks goes to former members of the Groves group who have helped me along the way: Dr. Cheng-han Yu, Professor Raghu Parthasarathy, Professor Sharon Rozovsky. Thanks to Professor Martin Forstner for starting this project and allowing me to take it over.

Thanks also to my family, friends and peers who have lent me their ears and their shoulders when I needed them most. Thank you mom and dad for all the delicate pressure you have put on me to do the best that I can do and thanks to Harriet for always giving me positive encouragement, even during my foulest moods.

Chapter 1

Introduction

1.1 Abstract

The cell membrane is a fluid bilayer composed of a complex mixture of lipids and proteins with characteristics of organization amongst the individual components. Membrane anchors or lipid anchors are tethers that localize proteins to membrane surfaces. These anchors are mainly composed of a combination of saturated acyl chains, unsaturated isoprenyl groups, glycosphosphatidylinositols, and basic amino acid residues. It is generally agreed that specific membrane anchors can target proteins to the proper subcellular membrane compartment, but there is debate as to whether membrane anchors can also participate in the lateral organization within a membrane.

Central to this debate is the concept of lipid rafts, which are generally defined as heterogeneous domains that compartmentalize cellular processes. The raft hypothesis predicts that certain membrane anchored proteins, depending on the saturation of the fatty acid, will partition into or be excluded from such domains, and that this sorting mechanism is necessary for proper cell functions. Without any direct evidence of such behavior, this topic remains contentious, even as more and more discussions are held in the context of lipid rafts. In order to move beyond this, it is necessary to understand what defines a lipid raft and whether or not this model is useful for predicting how a lipid anchored protein might sort in the membrane.

1.2 Lateral inhomogeneities in the plasma membrane

The plasma membrane is a complex mixture of lipids and proteins that self-assemble to form a bilayer. This bilayer is sometimes described as a two-dimensional fluid where individual particles can diffuse freely in the plane of the membrane.¹ The membrane itself serves two functions: it is a semi-permeable barrier that defines the composition inside and outside of a cell, and it is a regulatory scaffold for a myriad of enzymatic processes.² On the latter point, it is important to note that cell membranes are not entirely homogeneous and that within this sea of lipids and proteins, distinct inhomogeneous clusters or domains exist.³ These lateral inhomogeneities are markers for organization in the membrane and it is believed that this organization may be responsible for regulating the enzymatic reactions that occur at the membrane.^{4,5}

Much more is known about how molecules are transported across the membrane than about how molecules organize laterally in the membrane. The study of membrane organization has been incredibly challenging, because most methods perturb the membrane, which may disrupt or induce organization. Despite these challenges, membrane organization is inherently tied to various biological processes such as cell signaling and cell morphology and is of great interest to biologists.^{6,7}

In this chapter, I will review the current views of membrane organization and highlight the results that have led to our understanding of the membrane. Because the idea of membrane organization continues to change according to the methods used to study it, I will discuss where the model succeeds and where it is lacking. I will focus on the organization of membrane anchored proteins, since they are studied as markers of general membrane organization.⁸⁻¹⁰

1.3 Membrane Anchors

1.3.1 Membrane anchored proteins may be organized in the membrane

A great number of membrane proteins are tethered to the cell membrane via covalently bonded fatty acids. The combination of acylations (myristoylation, palmitoylation), alkylations (isoprenylation), and glypiations (glycosylphosphatidylinositol, GPI), along with polybasic amino acid residues, make up the majority of lipid anchors whose role, is to target otherwise soluble proteins to the membrane.¹¹ In early investigations of protein distribution, GPI anchored proteins appeared to be enriched in domains in the membrane.^{9,12} That led researchers to wonder if all lipid anchors play a role in the lateral sorting of anchored proteins.⁴ A number of studies have focused on this question, generally by studying how these anchored proteins, both the full-length and just the anchor domain alone, colocalize.¹³⁻¹⁵ Several methods have been used to observe how these molecules are distributed in the membrane, but interpretations have not converged. Early investigations have led people to believe that the saturation level of the lipid moiety is paramount in determining how these proteins organize, according to the lipid raft model, explained in section 1.4. However, there has been no incontrovertible evidence that anchors are responsible for determining the localization of anchored proteins in cells. In this section, I will introduce the major lipid moieties responsible for anchoring proteins to the plasma membrane; their chemical structures are depicted in figure 1.1.

1.3.2 GPI anchors exhibit specific localization

GPI refers to a class of glycosylphosphatidyl molecules that are all composed of fatty acids, a phosphatidylinositol group and a trimannosyl-non-acetylated glucosamine (Man₃-GlcN) core that is conjugated to the –COOH terminus of a variety of different enzymes and are only found on the exoplasmic leaflet of the plasma membrane. GPI anchors vary in composition of the fatty acid composition. GPI anchored proteins have a signal peptide that targets the polypeptide for translocation to the lumen of the endoplasmic reticulum where a GPI anchor is linked to the carboxyl-terminus of the emerging peptide by a transamidase. The anchored protein is shuttled through the various processing organelles and sent to the extracellular side of the plasma membrane.¹⁶ In polarized epithelial cells, GPI anchored proteins are almost exclusively trafficked to the apical side of the cell, and are not found in the basolateral membrane which is separated from the apical membrane by tight junctions and desmosomes.^{9,12}

1.3.3 N-myristoylation and S-acylation are believed to promote colocalization

On the cytoplasmic side, there is a larger diversity of anchors that is usually composed of some combination of different lipid moieties. Myristoylations are N-linked 14 carbon saturated fatty acids specifically linked to a N-terminal glycine of a translated protein with the consensus sequence: MGXXXS/T, by an amide linkage during translation by an N-myristoyl transferase (NMT).¹¹ Like farnesyl chains, N-myristoylation usually follows a two-signal rule when anchoring proteins, meaning that the myristoylation is usually insufficient to anchor a protein to a membrane and requires a second anchoring group, usually a palmitate or a polybasic cluster of amino acids that interact with the many acidic phospholipids in the inner leaflet of the plasma membrane. N-myristoylation is also believed to play a role in targeting

proteins, such as members of the Src family of kinases and other signaling molecules, to the plasma membrane rather than to the other areas of the cell.^{8,17}

Like myristoylations, palmitoylations are also saturated acyl chains, but are linked via thioester bonds to cysteines by palmitoyl acyl transferases (although there is evidence this can occur non-enzymatically). S-acylation, is a more general term for this process, suggesting a promiscuity in the types of acyl chains that might be linked to cysteines.^{11,18} There is no clear consensus sequence for palmitoylation, although it can occur at either termini and can accompany transmembrane proteins, suggesting that it may play a structural role or affect lateral localization in the membrane. Because of their saturation state, both myristoylations and palmitoylations are believed to be involved with directing anchored proteins to lipid domains with similarly saturated sphingolipids and cholesterol.^{10,17,19,20} These more condensed regions will be discussed more in the next section, 1.4.

1.3.4 Isoprenyl groups are unsaturated

Unlike acylations, prenylations are unsaturated, branched alkylations of usually 15 carbons (farnesylations) or 20 carbons (geranylgeranylations) linked to C-terminal cysteines by a thioether bond. There are specific enzymes, farnesyl transferase (FT) and geranylgeranyl transferase I (GGT I) which recognize the consensus sequence CaaX at the C-terminus (where C is cysteine, a is any aliphatic residue, and X is any residue); the peptide is cleaved between the cysteine and the aliphatic residue and the X residue determines which isoprenyl group is linked.⁸ Rab proteins have a specific GGT II which recognize a Rab binding protein to transfer two geranylgeranylations to Rab.²¹ Farnesyl and geranylgeranyl moieties are chemically similar to each other, although the farnesyl group obviously has a shorter penetration depth into the bilayer. According to conventional models, isoprenyls are not predicted to play a role in the lateral sorting of anchored proteins in the membrane.^{22,23} Members of the Ras family of proteins have a hypervariable C-terminus that gets farnesylated, and a second component of either a palmitoylation or a polybasic cluster of amino acids, which is responsible for targeting Ras to the correct subcellular compartment.^{20,24,25}

1.3.5 Lipid anchors are markers for membrane organization

The above mentioned lipid moieties are combined variously to form lipid anchors. According to the literature, GPI anchored proteins are usually implicated in clustering into domains, both in the plasma membrane, but also in the organelles, for proper trafficking to the apical side of polarized cells. Palmitoylations also appear to be markers for some sorting behavior according to the lipid raft model.^{10,13,26} However, this model is specifically dependent on the composition of the membrane and not only does the plasma membrane and subcellular membranes have different proportions of different lipids, the exoplasmic and cytoplasmic leaflet compositions of the plasma membrane are actively kept different.²⁷

With the ability to engineer proteins and to specifically label peptides with genetically encoded fluorescent proteins, researchers can study the membrane driven localization of the anchor without any protein-protein interactions by fusing truncated forms of an anchored protein to monomeric fluorescent proteins and observe their localizations by microscopy or spectroscopy.¹³ Consequently, these anchors are an ideal, non-invasive marker for membrane organization, since there are no enzymatic domains to interfere with native cell functions.

There is a wide belief in the field that the saturation level and length of the fatty acids will determine lateral sorting, but careful examination of the empirical evidence suggests that the membrane may behave in a more complex fashion.^{14,27-29} Regardless, lipid protein anchors are useful probes of membrane organization.

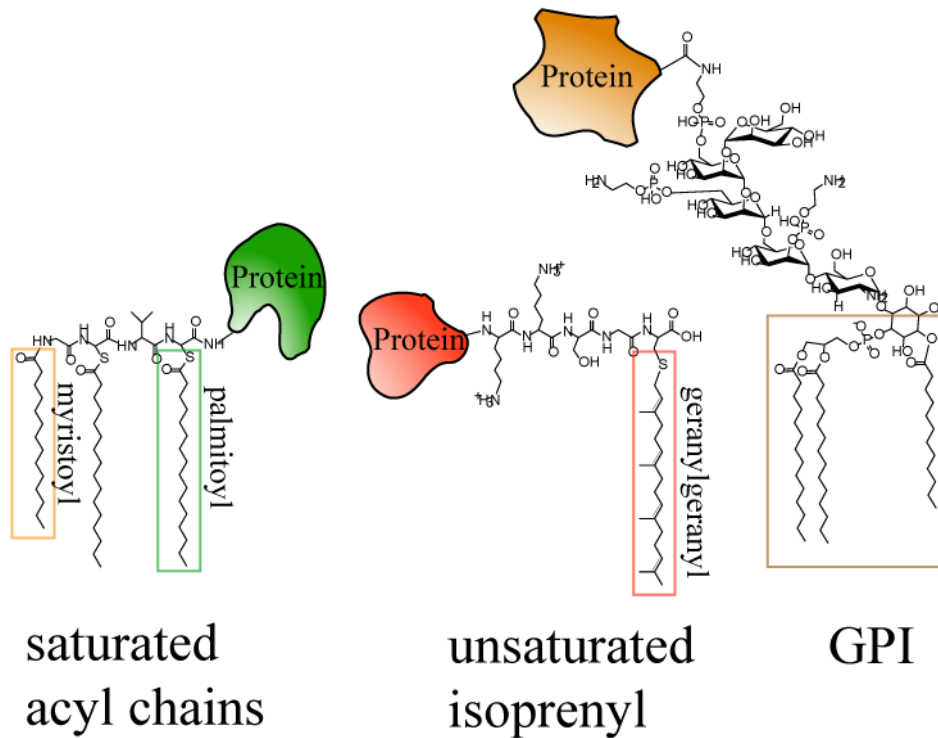


Figure 1.1 Membrane anchors are mainly composed of some lipid moieties and charged residues. Chemical structures of the common lipid moieties found in anchored proteins. Depicted from left, green cartoon protein has same anchor as lymphocyte cell kinase (LCK) with 1 myristoyl chain and 2 palmitoyl chain, red cartoon protein has anchor from RhoA kinase with a C-terminal geranylgeranyl lipid, and the orange cartoon protein has a generic GPI anchor. LCK and RhoA are discussed in more detail in chapter 2.

1.4 Lipid Raft Model

1.4.1 Lipid rafts mean different things

The term lipid raft has permeated into the biological lexicon, but the definition has been evolving. This has led to many different people having different ideas of lipid rafts. A recent symposium of biologists and biophysicists resolved to come up with a generalized definition of a lipid raft and sought to discard earlier ideas that had become inadequate.³⁰ However, this specific definition may not have been disseminated to the general scientific population, who may be laboring under an older model that is laden with previous misconceptions. A lot of the discrepancy arises from the different methods employed to study these inhomogeneities on the membrane.^{27,31,32} In this section I will outline several experimental observations that have been discussed in the context of lipid rafts.

1.4.2 Lipid rafts were first thought of as DRMs

Early discussions inferred organization from biochemical extraction of membranes. Similar to a protein pulldown assay, detergent solubilization of the membrane revealed regions of the cell membrane that were insoluble to detergent, which could be separated from the rest of the solubilized membrane and which reflected stable interactions between certain membrane components. These regions were referred to as detergent resistant membranes (DRMs) or detergent-insoluble glycolipid-enriched complexes (DIGs) and are enriched in sphingolipids, cholesterol, and certain types of proteins, such as glycosphosphatidylinositol (GPI) anchored proteins on the exoplasmic leaflet, acylated kinases on the cytoplasmic leaflet, caveolin, and some transmembrane proteins.^{4,9,12} These isolated DRMs were thought to represent physical domains in live cell membranes. Thus early studies of these lateral inhomogeneities, which were referred to as lipid rafts, equated DRMs with rafts, although immunofluorescent studies of proteins found in DRMs were never observed to partition into resolvable domains in cell membranes.^{27,30,32} This lack of direct observation has led to the requirement that lipid rafts are small, below the diffraction limit of light (~200 nm), but has also stirred up the most skepticism for the existence of such rafts. Since then, it has become generally accepted that DRMs do not necessarily represent interactions found in living cell membranes, since people have reported that detergents can disrupt transient organization in the membrane and induce stable interactions.^{30,33} Even though DRMs are not accepted as evidence of domains, many biologists who are not intimately involved in studying membrane organization, may still refer to DRMs as lipid rafts, which is one reason there is still confusion when the term lipid raft is used.

1.4.3 Model Membrane Phase Separation

Rather than looking at a complex system like the cell membrane, others have turned to model membrane systems with simplified, defined mixtures. At the time the lipid raft hypothesis was formulated, model membranes had been studied for several decades and much was already known about the chemical behavior of different lipid mixtures.³⁴⁻³⁷ An interesting phenomenon in both monolayer and bilayer experiments was the membrane's phase behavior. At critical points in the phase diagram, a bilayer with a ternary composition of saturated, unsaturated lipids, and cholesterol, could exhibit phase separation, where saturated lipids would form a gel-like liquid-ordered phase and separate from the rest of the more fluid, liquid-disordered phase. One of the driving forces for this entropically unfavorable behavior would be the hydrophobic mismatch that resulted from differences in the thickness between domains. This separation would produce line tension around the boundaries of these domains; coalescence of these domains would result in lower line tension and larger domains.^{31,38} Lipid dyes could be introduced into these systems to observe phase separation, since many lipophilic dyes would display preference for one domain over another. Proteins, as well, could be introduced into these systems and sometimes would also display preferences for particular domains.³⁹⁻⁴¹

The attraction for studying phase separated model membrane systems is that domains can be labeled with markers and are large enough to directly visualize by microscopy. Since DRMs were enriched in saturated sphingomyelin, cholesterol and saturated chain GPI anchored proteins, it seemed natural to assume that lipid rafts were like liquid-ordered domains and

formed as a result of phase separation of the lipids in the cell. Since this logical association, the term raft marker has been used to denote some liquid-order preferring protein. Many current studies equate a protein's raft partitioning preference to the degree to which it colocalizes with raft markers, such as the monoganglioside, GM1.⁴² Phase separated domains in model systems more closely resemble lipid rafts, because lipids can still freely diffuse in and out of the domains with a thermodynamic bias for a particular domain, which is unlike the stable domains derived from DRMs. As a result, lipid rafts are defined as heterogeneous regions in the membrane which form a more viscous and ordered domain.³⁰ Figure 1.2 depicts the generic understanding of a lipid raft.

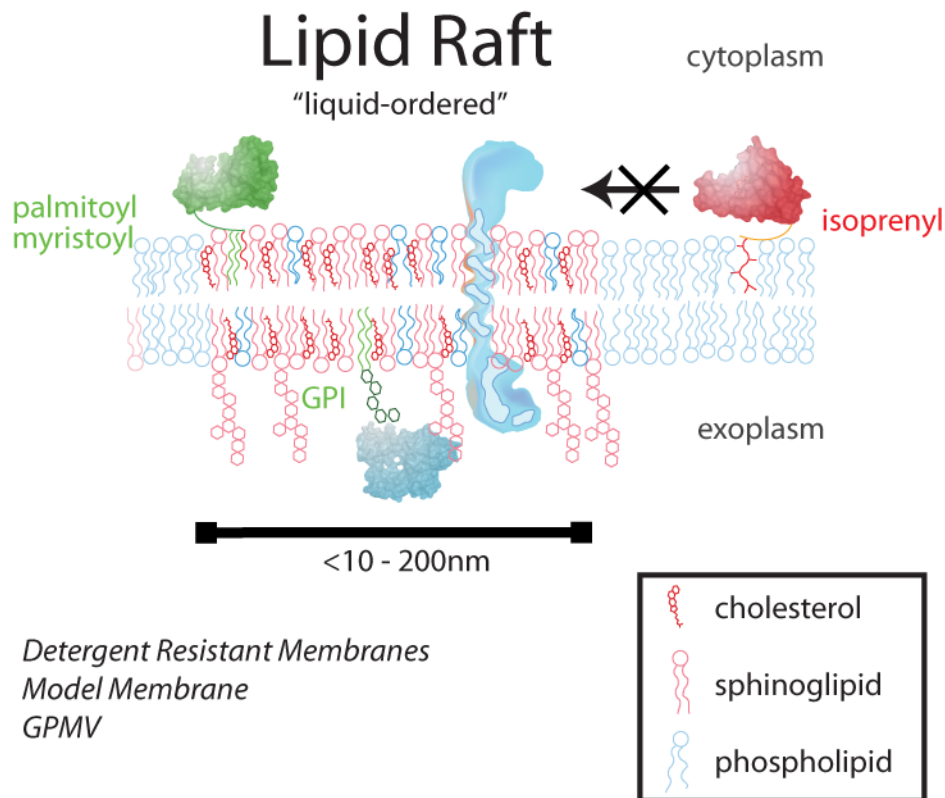


Figure 1.2. Cartoon depicting classical model of lipid raft. Lipid raft model was formulated from membrane extraction experiments and model membrane phase separation experiments. Lipid rafts are considered somewhat stable, small membrane domains that are enriched in cholesterol and sphingolipids, similar to the liquid order domain in liquid-liquid phase separation studies in model membrane systems. GPI anchored proteins and proteins with saturated acyl chain anchors (such as a palmitoyl group) are believed to preferentially partition into these liquid-ordered domains, whereas proteins with isoprenyls are believed to be excluded from these regions in the membrane. Transmembrane proteins in rafts are believed to couple the inner and outer leaflets of raft domains.

1.4.4 Phase separated vesicles do not represent domains in membranes

Two things are troubling about conflating model membrane phase separation with raft formation in living cells. The first is the difference in membrane composition; the reductionist approach may be useful in understanding the physical properties of lipids and proteins, but it

does not account for any possible complexity that may emerge from the much more complex mixture of molecules in the cell membrane.²⁷ However, this has been addressed with experiments involving giant plasma membrane vesicles (GPMVs), which are vesicles blebbed from real cell membranes. GPMVs were shown to phase separate and form large domains below physiological temperatures, similar to the phase separated domains in model membrane systems. These experiments demonstrate that the components of a cell membrane still adhere to physical principles and behave according to predictions. This does not address the second issue with model membrane systems, which is that the cell membrane is a system usually at steady-state, far from equilibrium. The cytoskeleton can interact with the membrane and impose order or disrupt interactions. Endocytosis and exocytosis constantly changes the concentration of proteins and lipids in the membranes. Even the lipid and protein composition of the two different leaflets of the plasma membrane are kept asymmetric, where the inner leaflet is enriched in charged phospholipids, and the outer leaflet has more sphingolipids and cholesterol.²⁷ These active processes could affect the organization, and cannot be modeled by vesicles. Despite this, many studies still refer to rafts in the cell membrane as liquid-ordered domains and raft markers are still considered liquid-ordered domain preferring molecules.

1.4.5 Better resolution of smaller features

Recent advancements in optical technologies and electronics have allowed more sensitive detection of individual molecules in the membrane at greater resolution. Being able to directly image molecules in the membranes of living cells would still offer the most conclusive picture of the membrane. Förster Resonance Energy Transfer (FRET) has become an oft-used technique for determining colocalization of particles. FRET only occurs at very close distances ($\sim < 10$ nm) and is a good measure of close interactions between proteins.^{43,44} An advantage to using FRET is that it is normally applied as a widefield technique and can be used to simultaneously observe heterogeneous levels of organization in the entire cell membrane. However, the drawback is that if one abides by the raft model, then lipids are capable of longer range organization than proximal protein-protein interactions. Consequently, it would be easy to miss longer range interactions. Furthermore, FRET relies on more stable interactions; it is difficult to distinguish between random collisional interactions from the interactions of a loose configuration of transiently associated proteins. In order to distinguish the difference, FRET relies on the *de novo* model that in random systems, increased fluorophore density leads to a linear increase in FRET efficiency, whereas actual coupling of a stable molecular system will saturate in FRET efficiency as density is increased.^{13,28} If the domain is not expected to be a long lived stable complex, then this data becomes very subjective to interpret. Studies of lipid anchors in different cell membranes have come back mixed. Some studies see evidence of raft model dependent clustering in epithelial cells, while other studies in T cells and fibroblast-like COS 7 cells see a random distribution of GPI anchors.^{13,28} These may be real differences, due to the nature of the membrane, or it may just be that FRET is not an entirely conclusive technique.

Superresolution microscopy and electron microscopy (EM) have also been used to tease out information about the structure of the membrane.^{45,46} These techniques can offer a snapshot of the actual architecture of the membrane. Electron microscopy was useful in establishing possible inhomogeneities early on, but suffered from cell preparation techniques that were potentially disruptive to native organizations. Superresolution fluorescent microscopy

techniques, which usually require long acquisition times, also use similarly harsh fixation techniques to prepare cell samples, although there has been some advancement towards imaging live, dynamic samples. Also, modern cryo-techniques are much improved over the last couple decades and it is possible to preserve the structure of a cell by vitrification for EM, although there is still a problem of labeling an anchor of interest efficiently with nano-gold labels such that it is representative of the distribution in the membrane. Additionally, in order to access the inner leaflet of a cell membrane, the membrane is usually torn from the cell to form plasma membrane sheets, which, like the GPMVs, are not ideal representations of the native form of the cell membrane.

1.4.6 Diffusional studies

Perhaps the most compelling descriptions of membrane organization come from methods that look at the diffusional behavior of membrane proteins or lipids. Looking at how molecules move in the plane of the membrane gives us information about the viscosity of the membrane and, consequently, the structure of the membrane. Diffusional studies benefit from sparse labeling and very non-invasive techniques. Single Particle Tracking (SPT), Fluorescence Recovery After Photobleaching (FRAP), and Fluorescence Correlation Spectroscopy (FCS) are used to directly observe how molecules move in the membrane.^{14,47-50} These approaches are not aimed at labeling and identifying static domains or structures in the membrane, but instead at looking at the movement of a probe to infer domains of different viscosity in the membrane.

SPT and FCS both rely on very sparse labeling of diffusive species in the membrane. Using high-speed cameras, SPT can plot out the diffusional tracks of anchored fluorescent proteins and determine if the protein displays random Brownian motion, directed transport, or some form of anomalous diffusion. By directly observing a single molecule's motion, one can determine if there are domains that would confine a molecule or obstruct a molecule's free diffusion.⁵¹ This technique was used to arrive at a different model of membrane organization, discussed in the next section, 1.4.7.

FCS looks at a population of single molecules at once. Fluctuation analysis of the fluorescence intensity of a labeled protein diffusing into and out of an excitation spot reports on the nature of the diffusion; the decay of the autocorrelation curve is related to the diffusion coefficient of the molecule and the heterogeneity of that diffusion. By varying the excitation spot size, probes in the cell membrane seem to exhibit free diffusion at small spatial scales and more anomalous diffusion at greater spot sizes.⁵⁰

The disadvantage, here, is that the diffusional models are all scale dependent and these approaches may miss any anomalous diffusion if the observed area or duration is less than appropriate. Still these limitations can be side-stepped by longer measurements or larger areas of observation. Techniques that only return bulk diffusion coefficient, such as FRAP, which photobleaches a spot and measures the diffusion coefficient by measuring the amount of time it takes for molecules to diffuse into the spot and replenish the photobleached area, are less useful in resolving heterogeneities in the membrane.⁵² FRAP, which is a very simple technique, may not be sufficient for teasing out more complex and heterogeneous organization in the membrane.

1.4.7 Picket Fence Model

SPT can be used to directly observe confinement zones in the membrane.^{47,53} Along with FCS, which can also observe confinement, it was shown that the membrane might be partitioned into innumerable domains by the actin cytoskeleton.⁵⁰ Researchers noticed that the diffusion was scale dependent, and that on the smallest scale, molecules could diffuse freely, but at greater scales, some anomalous behavior impeded such free diffusion.⁵⁴ The cytoskeleton lattice that forms the support of mammalian cell membranes is tethered to the membrane by interactions with membrane proteins. Commonly referred to as the picket-fence model, this model suggests that the more static actin network imposes long range order on the membrane, across several microns. However, it is believed that the actin cytoskeleton may also play a role in breaking up large uniform domains from forming. At the very least, the cytoskeleton is recognized to play a very influential role in membrane organization.

1.4.8 Does the raft model predict sorting?

With the diffusional studies, we get a more detailed view of the membrane without resolving exactly how the membrane is organized. There is a growing belief that lipid anchors themselves are not responsible for lateral sorting and organization of anchored proteins. Instead, it seems that proteins still require protein-protein interactions, perhaps in addition to lipid anchors, to determine its localization in the membrane. More recently the membrane raft model takes into account the role of protein-protein interactions.^{30,32} However, it must be asked what this revised model of membrane rafts tells us. As it stands, rafts are defined as small domains that are enriched in cholesterol and sphingolipids that serve some biological function in compartmentalizing proteins and lipids. Although the model no longer mentions phase separation as the sole driving force, many people still refer to lipid rafts as slightly more ordered liquid domains, which logically lead to binary outcomes: a molecule either prefers partitioning into the ordered domains or it doesn't, and those that do, should all colocalize. This result has never been observed in live cell membranes, but without this hypothesized phase separation behavior, the raft model no longer holds much relevance in predicting how molecules sort in live cell membranes. In fact, empirical evidence suggests that there is more heterogeneous organization in the membrane. This indicates that there is greater complexity in the membrane than is proffered by the raft model and we are starting to see some levels of this complexity.

Chapter 2 presents observation of membrane driven organization of specific lipid anchors in specific cell membranes, but not in a way predicted by the raft model. I argue that the membrane behaves with greater complexity than can be predicted by simplified model membrane systems. These studies employ Fluorescence Cross Correlation Spectroscopy (FCCS) a two color variant of FCS, which allows one to detect co-diffusion of two differently labeled anchors in live cells. Chapter 3 will detail some practical considerations for carrying out FCCS of fluorescently labeled membrane anchors in living cell membranes.

Chapter 2

Specific Lipid-Anchor Organization in Cell Membranes is Revealed by PIE-FCCS

2.1 Abstract

Many proteins are anchored to cellular membranes through various combinations of covalently attached lipid moieties. These modifications, along with polybasic regions of the proteins, are known to be essential for proper cellular localization. It has further been suggested that the anchors themselves may determine the lateral organization of lipid-anchored proteins in the plasma membrane. However, there is as yet no consensus on the spatial targeting characteristics of the various anchor types in living cells. In this study, we examine the dynamic colocalization of lipid anchored fluorescent proteins using pulsed-interleaved excitation fluorescence cross-correlation spectroscopy (PIE-FCCS) and fluorescence lifetime analysis. Specifically, we look at the colocalization of anchors from LCK (myristoyl, palmitoyl, palmitoyl), RhoA (geranylgeranyl), and K-Ras (farnesyl) proteins. The results reveal varying degrees of homogeneous colocalization of RhoA and LCK anchor types with no cross correlation between different anchors observed in Jurkat cell membranes. Fluorescence lifetime information compiled from the same data streams reveals essentially no Förster resonance energy transfer (FRET). Taken together, these observations suggest the lipid anchored fluorescent proteins are co-clustering with other native proteins or lipids in the membrane in an anchor specific manner.

2.2 Introduction

The cell membrane, primarily a two dimensional fluid lipid bilayer, is densely packed with a variety of proteins and conjugated polysaccharides that are laterally fluid in the plane of the membrane. Lipid anchors are commonly found on membrane proteins, and are known to facilitate trafficking to intracellular locations as well as regulate interactions between certain proteins.^{8,55} They also provide physical interactions necessary to tether many proteins to cellular membranes.⁵⁶ Lipid moieties that are attached as lipid anchors include isoprenyl groups, such as farnesyl and geranylgeranyl, and saturated fatty acids such as palmitoyl and myristoyl.⁵⁷ Lipid anchored proteins are often found to have multiple lipid modifications and/or basic amino acids that aid in stabilizing the protein-membrane interaction. Ras proteins are an example of a family of small GTPases that differ only in their hypervariable C-termini and lipid modification, and as a result are distributed amongst different organelle membranes and display differential sorting behavior in the plasma membrane.^{24,25,58} Swapping the anchors in other natively anchored proteins has been shown to disrupt protein function even when proper subcellular localization is maintained.¹⁵ These results suggest that anchors play a role in the differential lateral sorting of lipid-anchored proteins in live cell membranes.

Here, we study the organization of the anchor for the Lymphocyte Cell Kinase (LCK), an immediate downstream activator of T cell receptor activation during the immune response, the anchor for the small GTPase, RhoA, and the anchor for a member of the Ras oncogenic superfamily, K-Ras. Our study simply considers whether interactions between lipid anchors and membranes are capable of driving organization and whether different anchors are capable of differential sorting in the membrane. In order to study the lateral membrane partitioning behavior of lipid anchors, absent of any short-range protein-protein interactions, with high temporal and spatial resolution, we express truncated forms of our proteins of interest fused to either a red fluorescent protein, mCherry, or a green fluorescent protein, GFP, in live cells for

use with pulsed interleaved excitation fluorescence cross-correlation spectroscopy (PIE-FCCS). These truncated proteins contain only the anchor domain, which is the lipidation motif and the polybasic region of the peptide. (See figure 2.1) We employ PIE-FCCS to measure the degree to which these anchors colocalize in live cell membranes.⁵⁹ By expressing a green anchored protein and red anchored protein in each cell, we can do a pairwise comparison of our lipid anchors to look at homogeneous and heterogeneous colocalization.

Evidence from detergent resistant membranes suggests that palmitoylation strongly biases the partitioning of proteins into tightly packed domains, however, these assays require permeabilization of the cell membrane which disrupts the native organization and cannot be regarded as representative of the structure of the cell membrane.^{33,60-62} Model membrane systems also predict that lipid anchors will sort into domains based on their chemical structure. Giant unilamellar vesicles (GUVs) show that lipids and lipid anchors sort into liquid ordered (Lo) domains, consisting of ordered, tightly packed saturated lipid tails and cholesterol, and liquid disordered (Ld) domains, consisting of loosely packed unsaturated lipid tails.^{42,63,64} However, a simplified model membrane system does not reflect the complexity in the mixture of lipids and proteins from a cell membrane. A recent study in giant plasma membrane vesicles (GPMV), which are taken directly from cell membranes, shows inconsistent partitioning of lipid anchors between vesicles.⁴¹ The anchor of LCK, consisting of three saturated fatty acids partitioned into the Lo domain in some GPMVs, into the Ld domain in others, and still in others it resided equally in both.⁶⁵ While GPMVs maintain a similar membrane composition to live cells, they are removed from cytoskeletal interactions and active maintenance of the membrane composition, which may critically change lipid phase behavior. Finally, studies of lipid anchors in live cells further confuse the issue. Different Förster resonance energy transfer (FRET) studies have shown both clustering and non-clustering behavior of lipid-anchored fluorescent proteins in live cell membranes.^{13,28} On the other hand, studies using single particle tracking (SPT) and fluorescence recovery after photobleaching (FRAP), both of which observe diffusive behavior, found no evidence of anchors partitioning into stable domains.^{14,48} The general consensus taken from these results is that there is no clear model of how anchors organize in the membrane.^{27,32}

FCCS shows a definite correlation for two co-diffusing species regardless of their separation distance or orientation as long as they are both within the excitation area ($\sim 0.1 \mu\text{m}^2$).⁶⁶ PIE-FCCS provides cross-talk free cross-correlation and lifetime measurements from the same data stream allowing us to compare the amount of energy transfer (FRET) with the amount of cross-correlation.⁶⁷

We see varying levels of homogeneous colocalization in membranes of Jurkat cells transfected with either RhoA anchors or LCK anchors, but we see no heterogeneous colocalization between two different anchors. This finding suggests a minimum of two distinct domains, specific to each anchor, existing in a background of various other membrane components. This pattern was not consistent in the membrane of COS 7 cells, in which no colocalization was observed. In addition, we also notice no significant difference between the fluorescent lifetimes of GFP in different anchored pairs, regardless of the amount of correlation observed. This suggests that clusters are greater than ~ 10 nm and include other native membrane components.⁴³ Our results suggest that membrane organization of lipid anchors is anchor specific as well as membrane specific.

2.3 Materials and Methods

2.3.1 Cloning

Construction of truncated lipid anchor-fluorescent protein fusion genes:

Constructs of GFP-kRas-CT, mCherry-kRas-CT, mCherry-mGFP-kRas-CT in pN1 vector with a strong CMV_{IE} promoter were given as gifts from Dr. Nick Endres and Dr. John Kuriyan (UC Berkeley). Retroviral plasmids containing LCK-NT-mCherry, LCK-NT-GFP, mCherry-RhoA-CT, GFP-RhoA-CT were given as gifts from Dr. Björn Lillemeier and Dr. Mark Davis (Stanford). These genes were subcloned into the pN1 vector between the NcoI/NotI restriction sites. Polymerase chain reaction (PCR) primers and sequences of the genes can be found in Appendix A. All oligonucleotides were synthesized by Elim Bioscience (Fremont, CA) and sequenced by Elim Bioscience or the University of California Berkeley core DNA Sequencing Facility (Berkeley, CA)

Construction of His-tagged fluorescent protein (FP-His12):

Genes were cloned into the NcoI/XhoI restriction sites in the multiple cloning region downstream of a T7 promoter in the vector pET-28b(+) (Novagen). Genes for mCherry and mGFP were amplified by PCR and cloned into the NcoI/HindIII sites of pET-28b(+)-His12. mCherry-mGFP-His12 was constructed sequentially by first cloning mCherry into the NcoI/BamHI sites of pET28b(+) with an oligo cassette encoding a 12 X His-tag downstream of the fluorescent protein to generate pET-28b(+)-mCherry₁-His12. mGFP was then inserted into the BamHI/HindIII sites of pET-28b(+)-mCherry₁-His12 to produce pET-28b(+)-mCherry₁-mGFP₂-His12. All cloning was accomplished in *E. coli* XL1-Blue strain (Stratagene).

2.3.2 Protein Expression and Purification

FP-His12 protein was expressed in *E. coli* BL21 Star (DE3) strain (Invitrogen). Expression was induced during log phase growth with 1 mM Isopropyl β-D-1-thiogalactopyranoside (IPTG, Sigma), in 1 L suspension of Luria-Bertani bacterial media (Sigma) at 37°C for 3-5 hours. Cells were lysed by a freeze-thaw cycle, conventional treatment with 1 mg/mL lysozyme (Sigma) for 1 hour at 4°C in lysis buffer (40mM Tris pH 7.4, 275mM NaCl, 20mM Imidazole, 2% Protease Inhibitor Cocktail for His tag (Sigma)) and then by probe sonicator (Sonics & Materials Inc., VCX750). Samples were on ice during pulse sonication (5s ON/ 9s OFF, 150 seconds, amplitude = 35%, with a 3 mm stepped microtip). Lysate was clarified by addition of, and incubation with, nucleases (100 ng/mL RNaseA (Roche) and 25 ng/mL DNaseI (Roche)) and high-speed centrifugation (6,000 rcf) for 45min at 4° C then filtered through a 0.45 μm syringe filter. His-tagged proteins were purified by Immobilized Nickel Affinity Chromatography in a 1 mL His-Trap column on an AKTA Explorer (GE Life Sciences) and by Gel Filtration chromatography on a Superdex-100 HR Size Exclusion Column (GE Life Sciences) in Phosphate Buffered Saline, pH 7.4 (PBS, Gibco, Cellgro) and 20% glycerol (EMD). Purified proteins were concentrated with Amicon centrifugal filters and flash frozen in liquid nitrogen in aliquots and stored at -80° C.

2.3.3 Supported Lipid Bilayer Formation and Protein binding

Supported bilayers for empirical mapping of correlated states were made as previously described^{68,69}. 1,2-dioleoyl-sn-glycero-3-phosphocholine (18:1 (Δ 9-Cis) DOPC) and 1,2-dioleoyl-sn-glycero-3-[(N-(5-amino-1-carboxypentyl)iminodiacetic acid)succinyl] (18:1 Ni-NTA DGS) were purchased from Avanti Polar Lipids and stored at -20° C. 2 mol% and 10 mol% Ni-NTA DGS (with 98 mol% and 90 mol% DOPC, respectively) small unilamellar vesicles (SUVs) were prepared by sonication according to alternate protocol 1 in Lin *et al.*⁶⁸ Glass coverslip membrane supports (#1 Fisherbrand 25 mm round coverglass) are cleaned of organic contaminants by 10 min submersion in highly oxidizing Piranha etch solution (3:1 H₂SO₄:HOOH) thereby increasing the hydrophilicity of the support. 15 μ L SUVs are mixed 1:1 with 2 X Tris-Buffered Saline, pH 7.4 (TBS, Cellgro), and deposited on a clean, dry coverglass. Vesicles fuse to form a fluid supported bilayer on the coverglass. Coverslip and supported membranes are enclosed in a metal imaging chamber and the bilayer must remain hydrated in order to maintain fluidity. The water is exchanged for 100 mM NiCl₂, 2X TBS solution and incubated for 5min in order to charge the Ni-NTA DGS. The solution is washed with filtered H₂O and then exchanged with 5 mL of 1 X PBS. 2, 6, 10 mol% Ni-NTA DGS bilayers were incubated with ~3, 6, or 9 nM FP-His12 proteins in PBS for ~ 30-40 min, after which all unbound proteins are washed away by exchanging the solution with 10 mL of PBS.

2.3.4 Cell Culture/Transfection/Sample preparation

Mammalian cell cultures were obtained from Dr. Ann Fischer in the University of California Berkeley Tissue Culture Facility. Jurkat T cells were cultured in RPMI1640 medium (Gibco) supplemented with 1 mM sodium pyruvate (Cellgro), 100 μ g/mL Penicillin/Streptomycin (Cellgro), and 10% Fetal Bovine Serum (FBS, Atlanta Biologicals). Cells were passaged every two or three days by seeding ~ 10⁶ cells in 5 mL media in a T-25 cell culture flask and were disposed of after ~ 15 passages. COS 7 cells were cultured in Dulbecco's Modification Eagle's Medium (4.5 g/L glucose DMEM, Cellgro) supplemented with 1 mM sodium pyruvate, 2 mM L-glutamine, and 10% FBS and passaged 1:20 at ~ 95% confluency and disposed of after 20 passages.

Cells were transiently transfected either 1 or 2 days before the experiment. COS 7 cells are seeded at a density of 250,000 cells/ 9.6 cm² well in a 6 well culture plate in 2.5 mL reduced serum Opti-MEMI (Invitrogen) the day before transfection, while 10⁶ Jurkat cells in 2.5 mL Jurkat media are seeded in each well with 2.5 mL of culturing media on the same day as transfection. For transfection, 2.5 μ g plasmid DNA is added to 250 μ L Opti-MEMI, then 10 μ L Lipofectamine 2000 transfection reagent (Invitrogen) is added to this mixture and incubated at room temperature for 30 min. This is then added to cells in 6 well culture plates and incubated at 37° C, 5% CO₂ for ~ 12-36 hours before the FCCS experiment.

In order to image Jurkat cells, cell culture media was exchanged in 2 x 5 mL PBS, pH 7.4 pre-warmed to 37° C, by centrifuge (5 min, 250 rcf) and resuspended in 500 μ L Hepes Buffered Saline Solution (pH 7.2) pre-warmed to 37° C and deposited on poly-l-lysine coated #1 coverglass (cleaned as before, and with 0.01% poly-l-lysine (P-L-L, Sigma) solution deposited on coverglass surface for 30 min, then aspirated) enclosed in a metal imaging chamber. Cells are allowed at least 15 min in the incubator in order to settle and adhere to the P-L-L coated coverslips. COS 7 cells are washed with 2 mL prewarmed PBS, pH 7.4 and then lifted from the surface by 1 mL CellStripper™ (Cellgro) for 5-10 min, then neutralized with 500 μ L un-supplemented DMEM. Cells are centrifuged (5-10 min, 250 rcf) and the solution is

aspirated. Remaining cells are resuspended in 500 μ l un-supplemented DMEM, and added to P-L-L coated coverslips in imaging chambers and allowed at least 15 min in the incubator to adhere to the coverslips.

2.3.5 PIE-FCCS

FCCS measurements of lipid-anchored proteins in live cells were taken on a customized microscope setup. A Kr/Ar mixed gas laser (Stabilite 2018-RM, Newport Corp., Irvine, CA) provides a wavelength of 568 nm while a pulsed diode laser (LDH-P-C-485, PicoQuant, Berlin, Germany) provides a 479 nm wavelength at frequencies from 2.5 MHz to 40 MHz. For FCCS, the 568 nm and 479 nm lines are combined and coupled into a single mode optical fiber. The beams are decoupled, expanded, and directed via a custom polychroic mirror (Chroma Technology Corp., Rockingham, VT) into the optical path of the microscope (TE2000E, Nikon Corp., Tokyo, Japan). A 100X TIRF oil objective, NA 1.49 (Nikon Corp., Tokyo, Japan), focuses down the excitation beam. The fluorescence is collected through the same objective and passed through a custom notch filter (Semrock, Rochester, NY) to remove any reflected laser light. The emitted light is then passed through a 50 μ m confocal pinhole (Thorlabs, Newton, NJ) to limit collection of out-of-plane fluorescence. A 580 nm long pass beamsplitter then splits and directs the emitted light toward two avalanche photodiodes (SPCM-AQRH-16, Perkin&Elmer, Canada). Optical filters 550 nm short pass and 645/75 nm band pass (Chroma Technology Corp., Rockingham, VT) for the green and red channels, respectively, further select for fluorescently emitted light of the proper wavelengths. A time-correlated single photon-counting (TCSPC) card (PicoQuant, TimeHarp 200, Berlin, Germany) collects signal from the APD's through a router (PRT 400, TTL SPAD router, PicoQuant, Berlin, Germany) in the form of time-resolved data, which is used for fitting fluorescence lifetimes. The power of each laser was measured before entering the optical path of the microscope and was kept between 0.9 μ W and 1.5 μ W. Measurements were taken with the lasers pulsing at 10 MHz. The cw Kr/Ar beam is pulsed by passing through a pulsing electro-optic modulator (EOM). The pulsing of the EOM and the diode laser is controlled and synchronized by a pulse generator (Quantum Composers, 9530 Series). A delay of about 50 ns is set between the diode pulse and the EOM to ensure that the fluorescence completely decays between excitation pulses.

Cells were selected by looking at the epifluorescence with filter cubes suitable for GFP and mCherry, individually. A suitable cell would have similar intensity in the both channels. When taking FCCS measurements, we avoided areas of the cell from which we could see background from proteins inserted into membranes of organelles or intracellular vesicles. The bottom membrane of the cell was brought into focus and the PFS (The Perfect Focus System, Nikon Corp., Tokyo, Japan) maintained that focus throughout FCCS measurements. Three to five 15-second measurements were taken from each of three to five spots on a single cell, and three to five cells were observed per sample. The cell samples were kept at ambient temperature and atmosphere during data acquisition for no more than 1.5 hours.

2.3.6 Lifetime acquisition

Fluorescence data for lifetime analysis was acquired either simultaneously with FCCS data, or was acquired from separate samples (*e.g.* for cells expressing GFP-LCK only).

Lifetime histograms were constructed from 15 to 120 second traces, and were tail-fit with SymphoTime software (SymphoTime 5.1.3, PicoQuant, Berlin, Germany).

2.3.7 Data Analysis

PIE-FCCS data were time-gated as illustrated in figure 2.2 B to remove photons possibly resulting from spectral bleed-through using custom Matlab (The MathWorks, Inc) programs. The auto- and cross- correlation curves were calculated from the reconstructed intensity traces without the gated photons using a multiple-tau algorithm as discussed by Wohland *et al.*⁷⁰ Auto- and cross-correlation curves from a single spot were averaged before fitting. Curves that were calculated from intensity traces with large and irregular intensity fluctuations or resulting curves showing long and irregular decays indicative of large intensity fluctuations were discarded, as these irregularities cause artificially high amplitudes in the correlation curves and are usually the result of membrane fluctuations or diffusion of intracellular vesicles into the excitation area. Auto- and cross-correlation curves were fit by finding the average of the earliest ten points in order to get an accurate $G(0)$ value.

2.4 Results

2.4.1 Live cells express lipid anchored fluorescent proteins

Here we transiently transfect Jurkat and COS 7 cells with pairs of lipid anchored green- and red-fluorescent protein constructs. Transient transfections allow us to observe a broad distribution of densities of lipid anchored fluorescent proteins in a population of cells. As seen in figure 2.1, transfected cells imaged by epifluorescence show a homogeneous distribution of fluorescent proteins on the plasma membrane. The lipid anchor fluorescent protein fusions

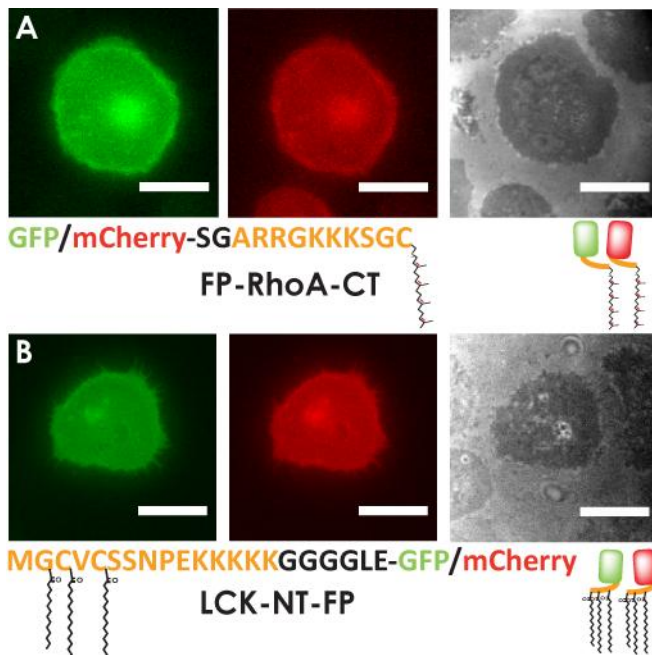


Figure 2.1. Epifluorescence of Jurkat cells expressing anchored fluorescent proteins shows homogeneous distribution in the plasma membrane. Green, red epifluorescent, and reflection interference contrast microscopy (RICM) images of Jurkat cells expressing (A) GFP-RhoA-CT and mCherry-RhoA-CT and (B) LCK-NT-GFP and LCK-NT-mCherry. Anchored fluorescent proteins are localized to the plasma membrane, and bright masses are due to intracellular organelles. RICM shows cell membranes are well adhered to P-L-L coated coverslips. Images are false-colored and the intensity scaled to show homogeneous distribution of anchored fluorescent proteins in the plasma membrane. The scale bar is 10 μm .

described here are similar to those used in previous studies.^{13,14,48,65,71} Because the native protein is not included in these chimeras, the localization and diffusion of the fluorescent lipid anchors are unaffected by any direct protein-protein interactions. Instead, the movement and colocalization of the fluorescent lipid anchors is a direct consequence of interactions between the lipid anchor and native components of the plasma membrane, including possible interactions between the basic residues of the peptide and lipid headgroups.^{65,72}

2.4.2 Relative correlation is measured by PIE-FCCS

Using PIE-FCCS we detect dynamic colocalization of GFP and mCherry lipid anchored constructs in live cells. This technique requires no fixation of cells or extraction of cell membranes, and measurements do not perturb the native organization of the membrane. We are unrestricted by the small, <10 nm, separation distance necessary for FRET as well as the >200 nm resolution of traditional optical microscopy. The observation of cross-correlation reports dynamic colocalization and requires no *a priori* knowledge of the spatial length of organization.

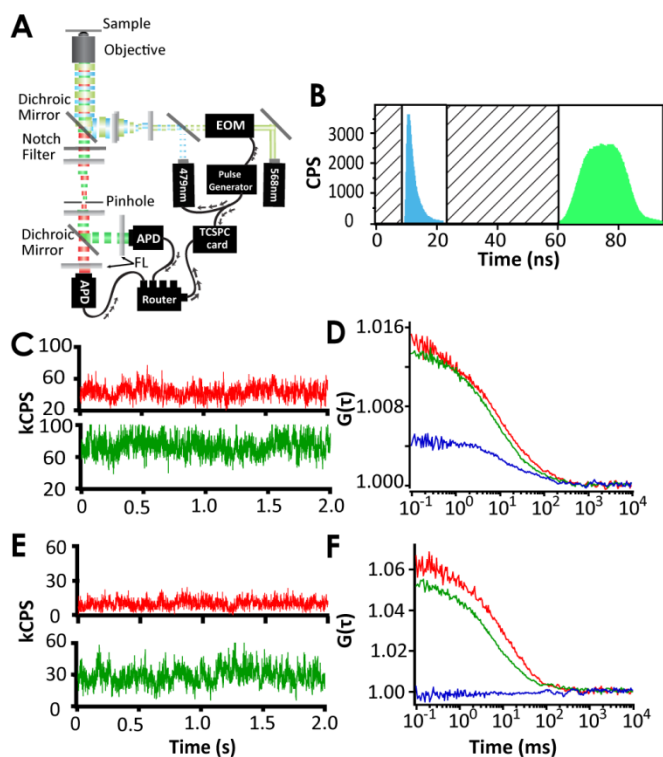


Figure 2.2. PIE-FCCS acquisition generates cross-talk free data. (A) Schematic of our PIE-FCCS microscope setup. (B) Arrival time (time-resolved) histogram of APD A (red) and APD B (green). Photons with arrival times within the diagonal lined boxes are removed before auto- and cross-correlation curves are calculated. (C) Intensity traces from APD A (red) and APD B (green) resulting from detected fluorescence from a bilayer sample with mCherry-mGFP-His12 exhibiting correlated diffusion. (D) Auto- (red and green) and cross-correlation curves (blue) calculated from the intensity traces in (C). (E) Intensity traces from a bilayer sample with mCherry-His12 and mGFP-His12 exhibiting uncorrelated diffusion. (F) Auto- and cross-correlation curves calculated from traces in (E).

Pulsed-interleaved excitation and proper data analysis ensure that we are seeing no artificial cross-correlation due to spectral bleed-through from the broad emission spectrum of GFP.⁵⁹ The time-tagged time-resolved (TTTR) data acquisition format records photons with their arrival time and time tag and allows us to acquire data for FCS, FCCS, and fluorescence lifetimes simultaneously.⁷³

Autocorrelation of fluctuating fluorescent signals (Figure 2.2 C and E) resulting from movement of fluorophores in and out of the excitation area is calculated by the normalized autocorrelation function in equation 2.1.

$$G(\tau) = \frac{\langle \delta I(t) \delta I(t+\tau) \rangle}{\langle I \rangle^2} + 1 \quad (2.1)$$

Where $\delta I(t)$ is the fluctuation in fluorescence intensity at time t , and τ is the lag time. Fluorescence cross-correlation is expressed similarly in equation 2.2, and gives the correlation between fluctuations from two different fluorescent signals.

$$G_x(\tau) = \frac{\langle \delta I_r(t) \delta I_g(t+\tau) \rangle}{\langle I_r \rangle \langle I_g \rangle} + 1 \quad (2.2)$$

Figure 2.2 D and F show two representative examples of auto- and cross-correlation curves from live sample Ni-NTA DGS bilayers, with mCherry-GFP-His12 (D) and mCherry-His12 + GFP-His12 (F).

While the $G(\tau)$ intercepts, $G_r(0)$ and $G_g(0)$, of the auto-correlation curves of red and green species are inversely proportional to the concentration of fluorophores in the excitation spot, $G_x(0)$ of the cross-correlation curve is directly proportional to the amount of dynamic colocalization or concentration of species with both red and green fluorophores.^{66,73} Here, we report a measure of cross-correlation in terms of F_{cross} as defined in equation 2.3.

$$F_{cross} = \frac{G_x(0)}{\min\{G_r(0)G_g(0)\}} \quad (2.3)$$

To better represent the amount of cross-correlation present in our transfected cells, we empirically map F_{cross} with physical standards on supported lipid bilayers as illustrated in figure 2.3 A. mCherry-His12, mGFP-His12 (top) and mCherry-mGFP-His12 (bottom) proteins are deposited on bilayers containing DOPC and 2%-10% Ni-NTA DGS. mCherry-His12 and mGFP-His12 diffuse freely and independently of one another on the same supported bilayer allowing us to measure uncorrelated diffusion by PIE-FCCS. Diffusion of mCherry-mGFP-His12 proteins on supported bilayers correspond to entirely correlated diffusion of red and green fluorescent proteins. Remarkably, increased density and, therefore, increased intensity of both fused and independent fluorophores results in decreased and even negative F_{cross} values as seen in figure 2.3 B. This decrease is linear with respect to the total intensity from both detection channels and is due to the dead time from the TCSPC acquisition card.⁵⁹

The TCSPC card has a longer dead time (~350 ns) than more conventional correlation cards or detection electronics.⁷⁴ Photons detected during a “dead time,” or when the TCSPC is processing a signal, are not recorded leading to an anticorrelation between GFP and mCherry at short lag times.⁵⁹ In our control bilayer measurements in figure 2.3, the effect becomes more dramatic as the intensity of the samples increases because the acquisition card is “dead” for a larger percentage of time. We have worked around this by empirically mapping our correlated and uncorrelated boundaries (Figure 2.3 B), and as we observe cells with total intensities

between 0 and 500 kCPS, the F_{cross} values fall between the negative and positive empirical boundaries of cross-correlation. These empirical values in the bilayer samples allow us to rescale our data to relative correlation values between 0 and 1 as shown in figure 2.4.

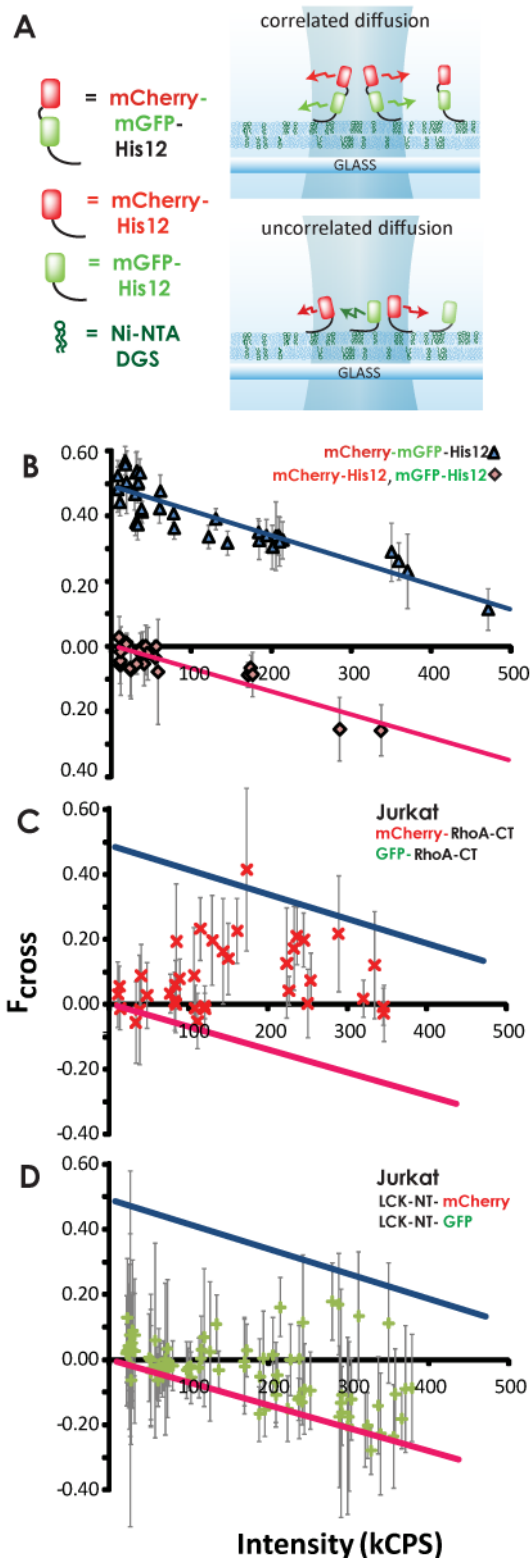


Figure 2.3. Empirical Mapping of Correlated States. (A) Schematic of mCherry-mGFP-His12 diffusing on a Ni-NTA DGS containing supported lipid bilayer representing the correlated state (top) and mCherry-His12 and mGFP-His12 diffusing independently on a supported lipid bilayer representing the uncorrelated state (bottom). (B) Scatter plot of F_{cross} versus intensity of correlated mCherry-mGFP-His12 (▲) and uncorrelated mCherry-His12 and mGFP-His12 (◆). Increased intensity comes from increased surface density of His-tagged fluorescent proteins. Decreasing cross-correlation with respect to intensity is due to TCSPC card dead time and is fit to a linear trend. (C-D) GFP-RhoA-CT/mCherry-RhoA-CT cross-correlation (x) and LCK-NT-GFP/LCK-NT-mCherry cross correlation (+) with respect to increasing intensity in Jurkat cells. Blue and magenta lines represent the linear fits of the empirically mapped cross-correlation states from (B). Error bars represent the standard deviation of G_0 at each spot.

2.4.3 Relative Correlation is dependent on density

A significant amount of cross-correlation is observed in Jurkat cells transfected with mCherry-RhoA-CT and GFP-RhoA-CT. This cross-correlation is a direct sign of membrane-mediated dynamic colocalization of RhoA anchors. Relative cross-correlation increases with increasing expression and intensity of anchored fluorescent proteins (Figure 2.4 row 2 column 2, data from 4 experiments, 11 cells). At low intensities, the relative correlation is not distinct from uncorrelated bilayer samples, but as we look at brighter cells, the relative correlation increases and approaches the value obtained from the positive correlation control bilayer samples. To translate intensity to an actual density of lipid anchored fluorescent proteins as shown in Figure 2.6 B and C, we divide the total intensity from each channel by the molecular brightness of mGFP-His12 and mCherry-His12 as obtained from the supported bilayer samples to determine the average number of individual fluorescent protein molecules in the excitation spot. The molecular brightness of mGFP-His12 and mCherry-His12 is obtained by fitting the auto-correlation curves with the 2d diffusional model in equation 4. According to this model, the intercept of the function at $\tau = 0$, $G(0)$ of the autocorrelation function is inversely proportional to the number, N , of diffusing species in the excitation spot. We then divide the total intensity from each channel by the N obtained from fitting.

$$G(\tau) = \frac{1}{N} \left(1 + \frac{\tau}{\tau_D} \right)^{-1} + 1 \quad (2.4)$$

Once we find the number of fluorophores in each spot based on intensity, we divide by the area of the excitation spot to get ρ . The excitation area is calibrated by fitting the auto-correlation curve for fluorophores of known diffusion constants and is $\sim 0.1 \mu\text{m}^2$.

2.4.4 Relative correlation is anchor specific

Examination of a different anchor pair, LCK-NT-mCherry and LCK-NT-GFP, shows less of a trend (Figure 2.4 row 1 column 1, data from 7 experiments, 28 cells). The relative cross-correlation values increase more slowly and are more spread across values from 0 to 1 at high densities.

In order to see if the different anchor types can partition into the same diffusing domains, we consider the pairwise relative correlation of LCK-NT-mCherry/GFP-RhoA-CT and mCherry-RhoA-CT/LCK-NT-GFP (Figure 2.4 row 2 column 1 and row 1 column 2, data from 5 experiments, 16 cells). In both cases, we see no cross-correlation regardless of density.

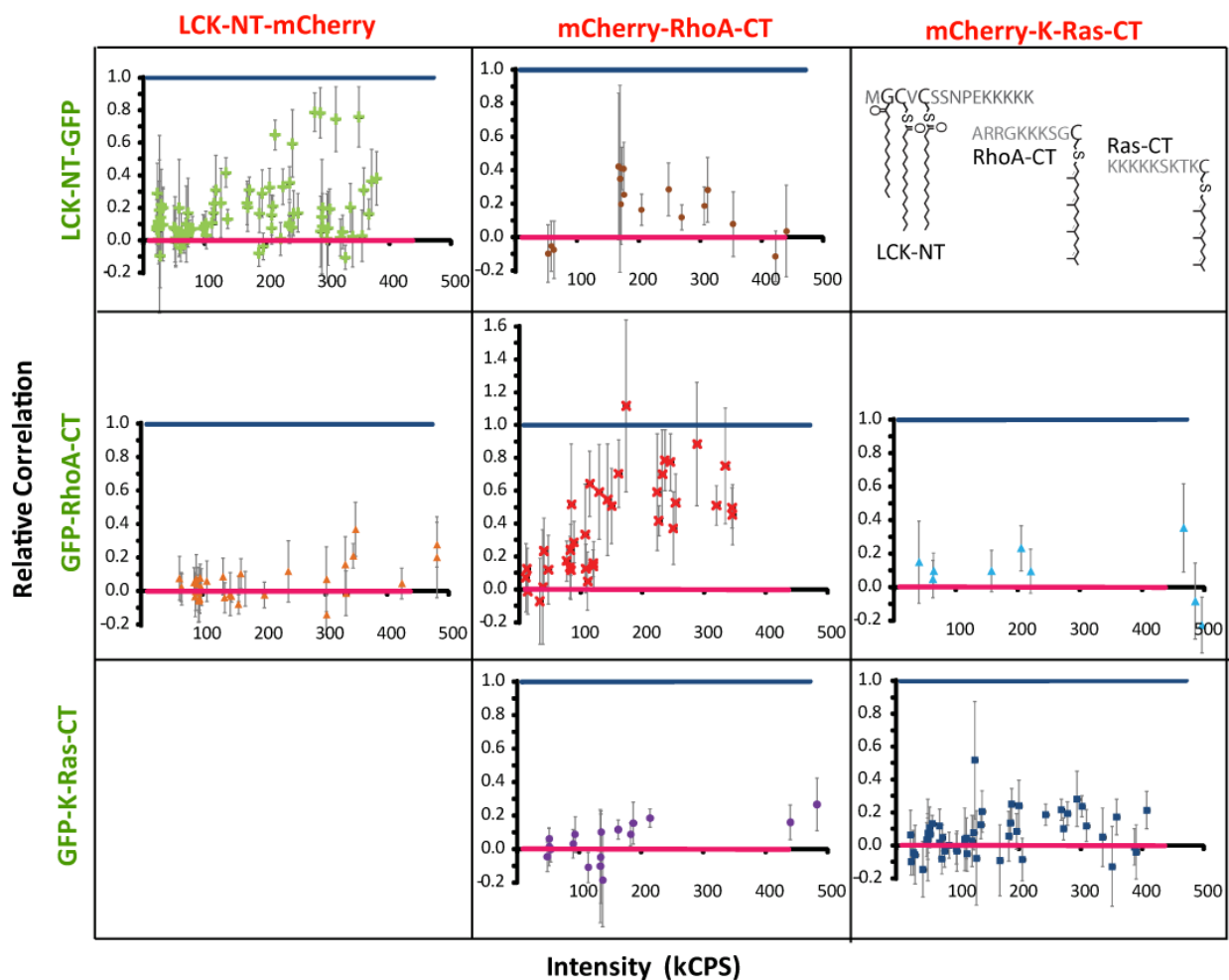
We also measure the relative correlation of the C-terminal farnesylated anchor of the Ras family kinase, K-Ras, which is chemically similar to the geranylgeranyl anchor of RhoA (see also chapter 2.7.1, SI Fig 1). Cherry-K-Ras-CT/GFP-K-Ras-CT FCCS measurements do not reveal significant cross-correlation within the range of intensities (Figure 2.4 row 3 column 3, data from 4 experiments, 13 cells). Similarly, the pairwise measurements of kRas-CT anchor with RhoA-CT anchor also do not exhibit any cross-correlation (Figure 2.4 row 3 column 2 and row 2 column 3, data from 3 experiments, 8 cells).

The lack of cross-correlation in the pairing of two different anchors tells us two things. First, the monotonic increase in RhoA anchor correlation and the increase in LCK correlation are not effects of having increased anchor density in the membrane, but are behaviors specific to

those anchors. The second is that these anchors organize orthogonally; RhoA anchors and LCK anchors do not partition into the same clusters.

Figure 2.4. Comparison of relative cross-correlation of different membrane anchors in Jurkat cells.

Normalizing cross-correlation to the empirically mapped correlated (1, blue) and uncorrelated (0, red) states for (top row, left to right) LCK-NT-GFP/LCK-NT-mCherry (28 cells) (◆), LCK-NT-GFP/mCherry-RhoA-CT (5 cells) (●), (middle row, left to right) GFP-RhoA-CT/LCK-NT-mCherry (11 cells) (▲), GFP-RhoA-CT/mCherry-RhoA-CT (11 cells) (×), and GFP-RhoA-CT/mCherry-kRas-CT (3 cells) (▲), (bottom row, left to right) GFP-kRas-CT/mCherry-RhoA-CT (5 cells) (●), GFP-kRas-CT/mCherry-kRas-CT (13 cells) (■) in Jurkat T cells. Error bars represent the normalized standard deviation of $G(0)$ for each spot.



2.4.5 Relative correlation is cell-specific

Finally, we compare the cross-correlation of the RhoA anchors and the LCK anchors in the membranes of epithelial COS 7 cells to our results in Jurkat lymphocytes, and notice that anchors do not organize in the same manner. In COS 7 cells we no longer observe clustering in the RhoA anchors (data from 3 experiments, 6 cells), nor do we see it in the LCK anchors (data from 3 experiments, 10 cells). These cross-correlation results tell us that the complexity of

membrane organization is specific for different cell types, and that membranes may organize differently based on membrane composition or cell function. (see chapter 2.7, SI Fig. 2)

2.4.6 Fluorescence lifetimes show no energy transfer

In order to examine local spatial organization, we measure the lifetime of the GFP-anchored proteins in our cross-correlation experiments as shown in figure 2.5. Shortened GFP lifetimes would be an indication of FRET between two anchors. There is a slight decreasing trend in lifetimes of all samples, including cells transfected with only a GFP-anchor and cells transfected with fused mCherry/GFP, as intensity increases, which can be attributed to the dead time effect of the TCSPC card. All cells transfected with a pair of GFP and mCherry anchors show GFP lifetimes similar to cells expressing only LCK-NT-GFP or GFP-RhoA-CT indicating no energy transfer due to FRET between mCherry and GFP. The exception is the fusion, mCherry-mGFP-KRas-CT, which shows strong evidence of FRET due to the short distance between the two fluorophores.

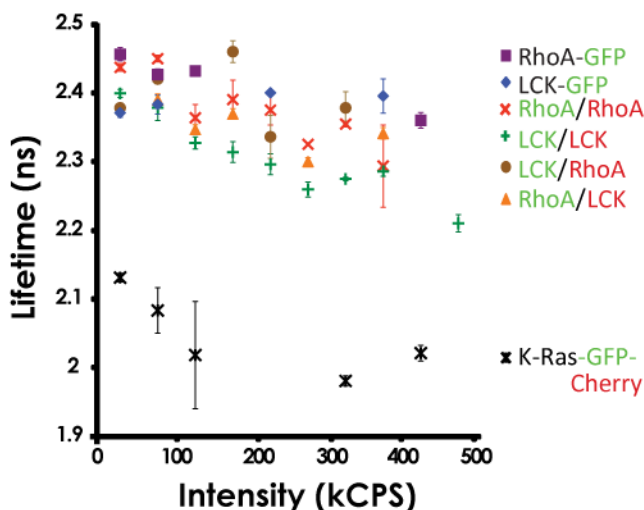


Figure 2.5. Fluorescence lifetimes do not show evidence of energy transfer. GFP fluorescence lifetimes decrease uniformly regardless of anchor type or anchor combination. Cells transfected with anchored GFP and anchored mCherry show the same decreasing trend with increasing intensity as cells transfected with only anchored GFP (Lck-GFP and RhoA-GFP). The striking difference in lifetime of the GFP when fused to mCherry in the single polypeptide K-Ras-GFP-Cherry, which we expect to undergo FRET, shows that none of the other anchored GFPs undergo significant energy transfer. Fluorescence lifetimes were fit, and the fitted lifetimes were binned into 50kCPS bins. The error bars represent the standard error of all points in each bin.

FCCS of our anchored fluorescent proteins gives us one picture of membrane organization, while comparisons of GFP lifetimes add greater detail to this picture. By pairing our co-diffusion studies with a look at very close molecular interactions, we begin to have an idea of the spatial dimensions of the organization. A lack of appreciable FRET in our cross-correlating RhoA anchors indicates that they are partitioning into clusters that are probably larger than ~ 10 nm in diameter.⁷⁵ We do not see energy transfer, even at higher densities, when there is a greater chance of having a cluster multiply labeled with red and green fluorophores. It is worth noting that FRET experiments alone would not detect RhoA anchor colocalization in this density range.^{27,48} This emphasizes the importance of using FRET alongside techniques that investigate the diffusive behavior of the species involved or are not limited to interactions within ~ 10 nm.

2.5 Discussion

We see from our results, that a density threshold must be overcome before any dynamic colocalization is detected. This tells us that the anchors partition into a pool of distinct, preexisting clusters present in the membrane.¹⁴ If anchors clustered strongly with one another or partitioned into large domains, we would expect to see significant cross-correlation at much lower densities. To put it another way, a finite number of clusters in the membrane is responsible for frustrating anchor cross-correlation until higher labeled anchor densities are reached. Remarkably, we see that both RhoA anchors and LCK anchors will distribute into clusters and that these clusters are distinct from each other.

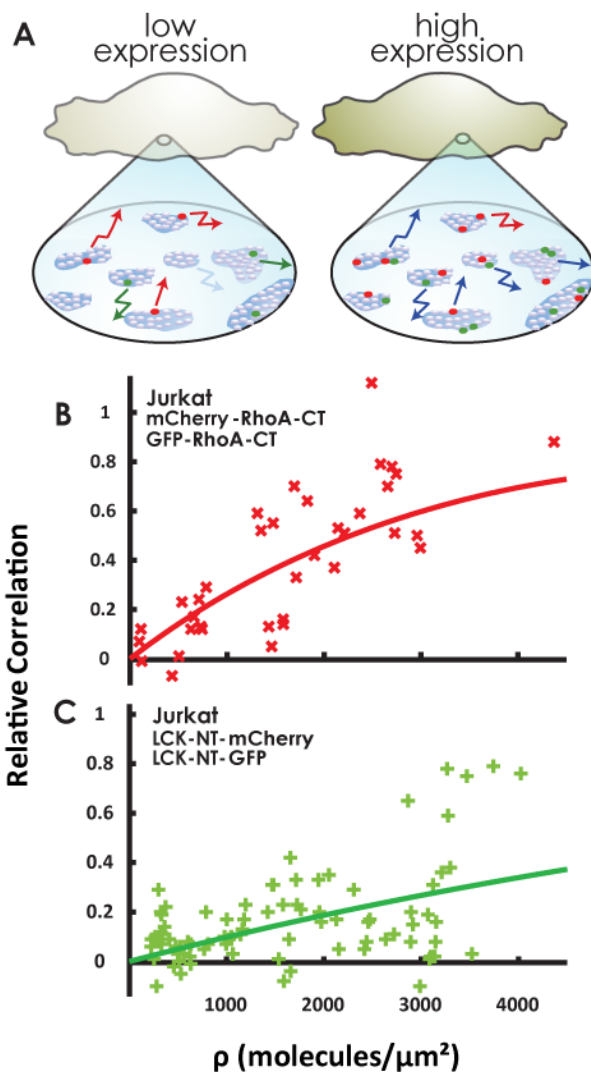


Figure 2.6. Physical Model of RhoA-anchor clustering. (A) Our model of RhoA anchored-fluorescent proteins sorting into pre-existing clusters. As expression levels increase, the likelihood of two or more RhoA anchored fluorophores partitioning into the same cluster increases according to a Poisson distribution and the likelihood of seeing at least one red and one green in the same cluster increases according to a binomial distribution. (B-C) Relative cross-correlation of (B) mCherry-RhoA-CT/GFP-RhoA-CT and (C) LCK-NT-mCherry/LCK-NT-GFP with respect to the total surface density of anchored fluorescent proteins in Jurkat cell membranes. The distribution of relative correlation is fit with our model to return the average number of clusters for each type in the cell membranes, 1640 clusters/ μm^2 (R-square = 0.5934) and 4821 clusters/ μm^2 (R-square = 0.2358) for (B) and (C) respectively.

We can consider our anchored fluorescent proteins as probes in the membrane and describe this trend of increasing cross-correlation with increasing intensity by a probability distribution of observing at least one red and one green anchor probe present in a cluster. We start by noting that the labeled anchors are distributed randomly among the clusters, so the

probability of one cluster having N probes follows the Poisson distribution, where $\langle N \rangle = \rho/n$ with ρ as the number of probes per μm^2 , and n as the number of clusters per μm^2 :

$$P_{cluster}(N; \langle N \rangle) = \frac{\langle N \rangle^N e^{-\langle N \rangle}}{N!} \quad (2.5)$$

By choosing a probe at random, the probability distribution for N other labeled anchors in the same cluster is scaled by the number of labeled anchors in the cluster.

$$P_{probe}(N; \langle N \rangle) \propto N \frac{\langle N \rangle^N e^{-\langle N \rangle}}{N!} \quad (2.6)$$

The normalized probability distribution for N for the cluster in which the chosen probe resides follow.

$$P_{probe}(N; \langle N \rangle) = \frac{N}{\langle N \rangle} \frac{\langle N \rangle^N e^{-\langle N \rangle}}{N!} \quad (2.7)$$

We now consider that in order to see cross-correlation, at least one of the other probes in the cluster must be the opposite color of the chosen probe. This probability that at least one of the $(N-1)$ probes is of the opposite color is given by,

$$P_{cross}(N) = 1 - \left(\frac{1}{2}\right)^{(N-1)} \quad (2.8)$$

Finally, the total probability that any given probe is in a cluster with at least one other probe of the other color is given by summing up all of the possible ways this can happen:

$$P_{total} = \sum_{N=0}^{\infty} \frac{N}{\langle N \rangle} \frac{\langle N \rangle^N e^{-\langle N \rangle}}{N!} \left(1 - \left(\frac{1}{2}\right)^{(N-1)}\right) \quad (2.9)$$

In effect, P_{total} is the probability of observing cross-correlation at a particular probe density in the membrane, which is the same as our measure of relative correlation.

In figure 2.6, we have converted intensity to density using the molecular brightness of GFP and mCherry from control bilayers, and fit the RhoA clustering data to the probability distribution shown in equation 2.9 to find the average number of clusters where $\langle N \rangle = \rho/n$. Fitting the RhoA anchor data, we find a minimum of 1640 clusters per square micron ($R^2 = 0.593$). This result represents a minimum value because the intensity of brighter samples is probably under-detected due to the dead time of the TCSPC card, and the actual density may be greater.

We are limited by our method from seeing higher membrane densities, but in the case of LCK-NT-mCherry/LCK-NT-GFP cross-correlation, we catch a glimpse of the beginning of an increasing trend similar to that which we see in the case of the RhoA anchor. The best fit of our probabilistic model to the LCK cross-correlation values returns a cluster density of ~ 4821 clusters per square micron ($R^2 = 0.2358$), on average. These results show that partitioning into large domains is not the dominating behavior of LCK anchors. Instead, the clusters they

partition into are very numerous and probably small. This is in stark contrast to reports that the full-length LCK proteins colocalize into large T cell receptor signaling microdomains during T cell activation.^{14,26,76,77} Previous results suggest that the LCK anchor will sort into clusters regardless of T cell activation.^{13,78,79}

Based on our observations, we present a more complex picture than is predicted by general models of membrane organization. Although much research has advanced the understanding of membrane organization beyond stable micron-scale phase-separated lipid domains known as lipid rafts, liquid-ordered and liquid-disordered phase separation is still often referenced as the primary mechanism of sorting of membrane components.^{4,9,12,71} According to this lipid raft model, anchored proteins with saturated acyl chains, such as the LCK anchor, are expected to cluster into raft domains, while isoprenylated molecules like the RhoA anchor would be excluded to the surrounding disordered phase with no apparent clustering.^{13,80-82} Here we show the existence of two distinct, non-overlapping domains that LCK anchors and RhoA anchors recognize in a background of perhaps many other protein clusters in the membrane of Jurkat cells. This complexity extends to the differential sorting between the RhoA and K-Ras anchors due to their subtle differences. Our observations, and many previous studies, demonstrate that the complexity from the interactions between all membrane components in addition to interactions with the cytoskeleton and intracellular proteins cannot be fully described by an organizational scheme driven by binary phase separation.^{14,58}

It is also important not to conflate the observations made in different membrane systems. The models of membrane organization derived from GPMVs and model membranes, which are by default at equilibrium, do not predict the behavior seen in living cells maintained at a non-equilibrium steady state. A number of intracellular processes such as cytoskeletal interactions and endocytosis dynamically affect the composition and tension of the plasma membrane. Furthermore, different living cells can exhibit different organizational behaviors, as we see of the RhoA anchors in COS 7 cells, with respect to the anchors in Jurkat cells.

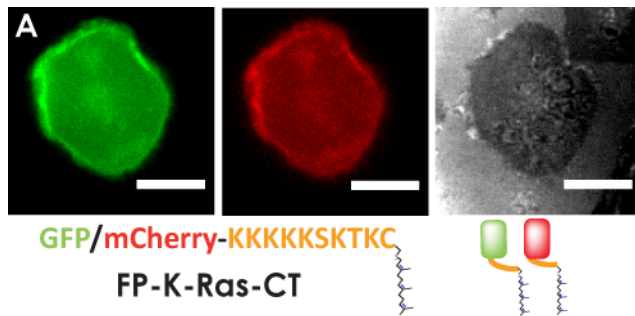
PIE-FCCS has allowed us to see a small window of what must be a complex and highly specific organizational scheme of the live cell membrane. The intensity requirements and limits of PIE-FCCS do not allow us to extend our measurements to more dense samples, but we clearly see that interactions between anchors and the membrane do cause differential sorting of anchors, and that simple binary phase separation does not explain the orthogonal nature of this differential sorting.

2.6 Acknowledgements

The authors would like to acknowledge Il-Hyung Lee and Michael Coyle for contributions of Matlab analysis scripts and Dr. Wan-Chen Lin for helpful FCS/FCCS discussion. The authors would also like to thank Ann Fischer from UC Berkeley Tissue Culture Facility for obtained mammalian cell cultures, Dr. Nick Endres and Dr. John Kuriyan for K-Ras anchor containing plasmids, and Dr. Björn Lillemeier and Dr. Mark Davis for access to LCK and RhoA anchor containing plasmids. Finally, the authors would like to thank Howard Hughes Medical Institute and the Department of Energy for funding and support.

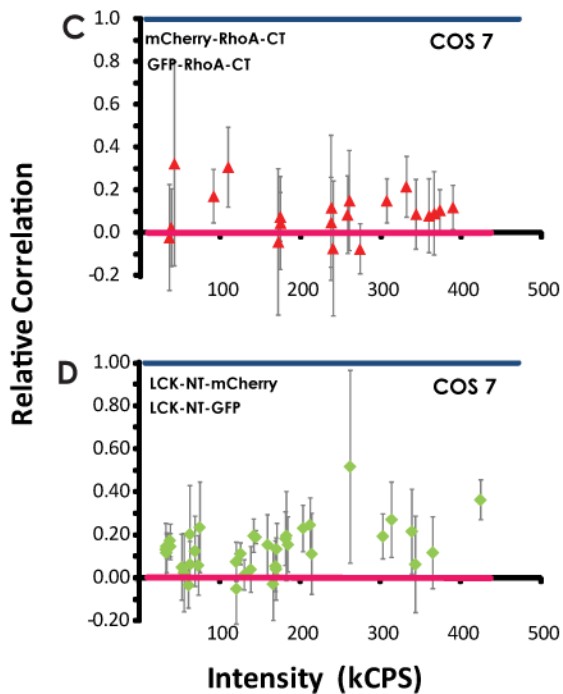
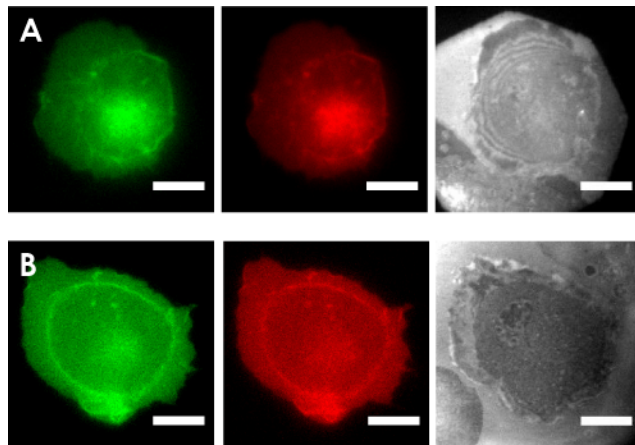
2.7 Supporting Information

SI Figure 1. Epifluorescence of Jurkat cells expressing K-Ras anchor fluorescent fusion protein shows homogeneous distribution in the plasma membrane. Green, red epifluorescent, and reflection interference contrast microscopy (RICM) images of Jurkat cells expressing (A) GFP-K-Ras-CT and mCherry-K-Ras-CT. Images are false-colored and the intensity scaled to show homogeneous distribution of anchored fluorescent proteins in the plasma membrane. The scale bar is 10 μm .



SI Figure 2. Epifluorescence of COS 7 cells and comparison of relative cross-correlation of different membrane anchors in COS 7 cells. Green, red epifluorescent, and reflection interference contrast microscopy (RICM) images of COS 7 cells expressing (A) GFP-RhoA-CT and mCherry-RhoA-CT and (B) NT-LCK-GFP and NT-LCK-mCherry. Images are false-colored and the intensity scaled to show homogeneous distribution of anchored fluorescent proteins in the plasma membrane. The scale bar is 10 μm .

Normalizing cross-correlation to the empirically mapped correlated (1, blue) and uncorrelated (0, red) states for (C) GFP-RhoA-CT/mCherry-RhoA-CT (6 cells) (\blacktriangle) and (D) LCK-NT-GFP/LCK-NT-mCherry (10 cells) (\blacklozenge) in COS 7 cells. Error bars represent the normalized standard deviation of $G(0)$ for each spot.



Chapter 3

Practical considerations for PIE-FCCS of lipid anchors in live cells

3.1 Abstract

PIE-FCCS requires relatively low excitation powers and very low concentration to perform. Fluorescent proteins are extremely useful, genetically-encoded markers of molecular location in a cell. Taken together, two color PIE-FCCS of proteins of interest fused to fluorescent proteins is an ideal, non-invasive method for studying fast dynamics in living cells. However there are some number of practical issues to consider before embarking on these experiments, both on the biology side and the spectroscopy side. An important matter to consider is the expected range of densities to be measured and whether or not this overlaps with the ideal range for PIE-FCCS. In this chapter I will highlight possible difficulties and limitations associated with studying anchor organization in living cells by PIE-FCCS.

3.2 Expression Level

3.2.1 Density Range

FCS and FCCS work best at very low concentrations of fluorophores – the technique relies on being able to temporally resolve fluctuations from several diffusing fluorescent species. An ideal density is ~10-100 molecules in the laser excitation spot at any time, which would work out to a concentration of ~30-300 per femtoliter (~50-500 nM) or a surface density of ~100-1000 molecules per square micron, in 2 dimensions. However, the results reported in chapter 2 indicate that noticeable cross-correlation of the fluorescently labeled RhoA-CT anchors does not occur until we detect ~2000 fluorescent molecules per square micron. (See figure 2.6) We begin to run into the limitations of our system at these densities. FCS and FCCS is less ideal at high densities, since the amplitude of the autocorrelation function, which is inversely proportional with concentration, becomes too small to accurately measure.⁷⁴ Consequently, we are only able to see the tail of a trend in cross-correlation for the LCK anchors within this window of observation.

Concentration dependent studies are not uncommon and FCCS can be used to study concentration dependent behaviors. For example, we can use FCCS to measure the homo-binding of two differently labeled species. In a tightly focused excitation spot (0.2 fL), if the K_d of this reaction is strong, $\sim 3 \times 10^{-8}$ M, then we would see 50% binding at that concentration, which comes out to ~8 particles of each color, and on average, we would see 25% cross-correlation.⁷³ If the affinity was weaker by 2 orders of magnitude, we would not see half-max binding until >1000 molecules. However, it gets more complicated *in vivo*, because there are various competing interactions that can frustrate cross-correlation, such that cross-correlation is not detected until at much higher densities of fluorophores. There is a density threshold that must be overcome before we can detect cross-correlation of RhoA lipid anchors in the experiments in chapter 2, which is dependent on the number of endogenous clusters in Jurkat cell membranes that the lipid anchor must partition into. With no *a priori* knowledge of the number of clusters present in a cell, we are required to explore different density regimes.

3.2.2 Different Expression Systems

Different cell types require different expression systems, and to a small extent these expression systems can attenuate the expression level. If the over-expression of the protein is toxic to cells, then inducible promoter constructs can be used, although the attenuation level is very coarse, and usually operates in a binary manner. Common inducible expression systems include the tetracycline inducible promoter, such as the TetOn™ or TetOff™ system from Clontech, or the Proteotuner™ system, also from Clontech, which adds a destabilization domain to the terminus of the protein that immediately targets the protein for proteolysis, but can be rescued by titrating a membrane permeable small molecule. In both cases, protein expression/rescue must be induced 4-12 hours before the experiment. Furthermore, in order for this to be reproducible, it is usually recommended that a stable cell line be generated. Innate expression levels can be selected for by fluorescence activated cell sorting (FACS) of individual cells and monoclonal populations can be expanded, but this takes several weeks to months to establish, while transient transfections usually generates a broad distribution of expression levels in a cell population and takes a day or two.

Over-expression of truncated lipid anchor fluorescent proteins in chapter 2 does not appear to be toxic to cells since the anchors and fluorescent proteins should not have any enzymatic activity. However, at high densities, many of the intracellular organellar membranes are decorated with a lot of fluorescence and there appear to be inclusion bodies from the abundant protein expression. This does not affect the morphology of the cell nor does it affect the heterogeneous distribution of fluorescent anchors on the plasma membrane.

While we explored some of the expression systems mentioned above, we settled on a strong constitutive promoter CMV_{IE} from the PN1 vector (from Clontech). This provided a broad range of expression levels in a transiently transfected population. The original retroviral plasmids that we received as gifts from Dr. Björn Lillemeier and Dr. Mark Davis (Stanford University) could be transiently transfected into our cells (Jurkat, HEK, COS 7) which would have some basal level, leaky expression and would also satisfy very, very low density measurements. We have found the complement of these two expression systems sufficient for exploring a broad range of densities. Details of the cloning and construction can be found in chapter 2.3.1

3.3 Cell type

3.3.1 Different cell types have different membranes

Chapter 2 reports differences seen in organization of lipid anchored proteins in the plasma membrane of different cell types: Jurkat leukemic T cells and fibroblast-like COS 7 cells. We are interested in examining the heterologous expression of our lipid anchor-fluorescent protein constructs in different cells in order to determine if membrane organization was universal amongst different membranes. We have also transiently transfected our anchors into several common tissue culture lines: the fibroblast-like line HEK 293T, the epithelial line MDCK, the fibroblast lines NIH-3T3 and Swiss-3T3, and CHO (See figure 3.1). We found COS 7 and Jurkat cells the easiest to culture, transfect, and image. COS7 cells are generally very large (~50µm diameter). When plated onto a poly-L-lysine coated coverslip, the cell is

flattened out like a fried egg and presents a large surface for imaging. It is possible to image COS 7 cells growing in culture rather than replating them on a poly-L-lysine coated coverglass, but the extracellular matrix adds some autofluorescent noise to the FCCS measurements. Jurkat cells, on the other hand, are small (~20 μm in diameter), but are very easy to culture and are known to exhibit a great deal of signaling activity at the membrane. Also, because they are not adherent cells, they must be plated on a poly-L-lysine coated coverslip in order to be imaged.

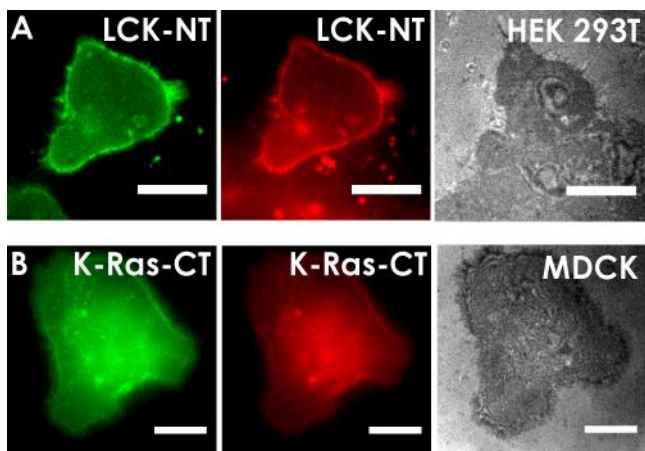


Figure 3.1. HEK 293T and MDCK cells expressing anchored fluorescent proteins. Green, red epifluorescent, and reflection interference contrast microscopy (RICM) images of (A) HEK 293T cells expressing LCK-NT-GFP and LCK-NT-mCherry and (B) MDCK cells expressing GFP-K-Ras-CT and mCherry-K-Ras-CT. Cell membranes are well adhered to P-L-L coated coverslips. Images are false-colored and the intensity scaled to show homogeneous distribution of anchored fluorescent proteins in the plasma membrane. The scale bar is 10 μm .

3.3.2 Notes on sample preparation

Cell culture details can be found in chapter 2.3.2. One thing to note is that transfection with a transfection reagent tends to be toxic to cells, so the shorter the duration of exposure to transfection reagents, the healthier it is for the cells. Cells are usually transfected for a minimum of 12 hours, before media is removed and the cells are placed in imaging buffer (for Jurkat) and imaging media (for COS 7) cells. Also trypsin was not used to lift the COS7 cells from the surface because trypsinization of membrane proteins may be a harsh treatment and may affect membrane organization. Cellstripper™ (Cellgro) is an EDTA based solution that chelates the cations that are necessary for cell adhesion. If imaging GPI anchored proteins, it is absolutely necessary not to use trypsin when preparing samples for imaging.

3.4 Empirical states of Correlation

3.4.1 Cross-correlation values should be mapped to known physical states

When using FCCS to detect colocalization of two molecules in a cell, it is necessary to map that behavior to known correlated states. The best way to do this would be to selectively measure cross-correlation of molecules on a two-dimensional surface where the state of colocalization is known. Here we have a supported lipid bilayer presenting a small (2-10 mol%) amount of Ni-NTA labeled headgroup lipid as a platform for his-tagged fluorescent proteins to strongly bind to and diffuse around freely. To match the uncorrelated states, a bilayer with equal numbers of mGFP-His12 and mCherry-His12 is presented. To match the correlated state, a bilayer presenting a fusion protein of mCherry-mGFP-His12 is presented.

Details for preparing supported bilayers and for adhering his-tagged proteins to the bilayer can be found in Chapter 2.3.3

3.4.2 Protein “freshness” is critical in *in vitro* experiments

Proteins are in phosphate buffered saline, pH 7.4, 20% glycerol and flash frozen in aliquots. Aliquots of GFP are thawed and used for < 2 weeks, stored at 4°C, before the protein begins to precipitate out of solution. Once GFP begins to precipitate, large fluorescent densities appear on the bilayer and cannot be used. Analytical FPLC shows obvious aggregates in solution, but protein oriented on a bilayer does not necessarily behave the same as protein diffusing freely in solution. The homogeneity of the fluorescence on a bilayer is the best evidence of the “freshness” of the protein. Figure 3.2 shows examples of “good” bilayers (A and B), where proteins appear homogeneously distributed, and “bad” bilayers (C and D), where large aggregates are obvious from epifluorescent images.

Details about the cloning of the His-tagged fluorescent proteins can be found in chapter 2.3.1 and details about protein expression and purification can be found in chapter 2.3.2.

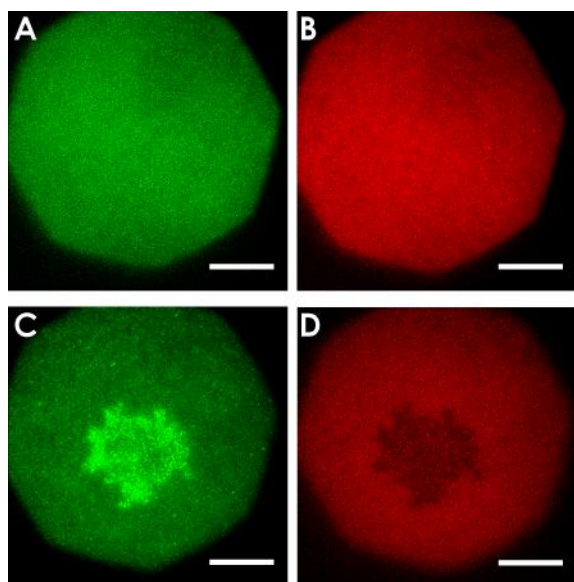


Figure 3.2. Example of good and bad bilayers (A and B) 2% Ni-NTA DGS bilayer with mGFP-His12 and mCherryHis12 bound to the bilayer should look homogeneously distributed by epifluorescence for both (A) GFP-His12 and (B) mCherry-His12. (C and D) “Unfresh” proteins, particularly the GFP, and old vesicles will form aggregates or defects on the bilayer. GFP is aggregated in (C) and mCherry is excluded from aggregated mass in (D). These epifluorescent images are false colored and intensity has been scaled to show distribution of fluorescent proteins on the bilayer. Octagonal outline is from partial closing of field aperture and scale bar is 20 μm .

3.5 FCCS

3.5.1 FCS/FCCS is used to study a number of dynamic processes

FCS of fluorescence in cell membranes is becoming more commonplace and has shown itself to be useful for characterizing the structure of the membrane by determining the diffusive behavior of proteins and lipids in the cell membrane. Two color-FCCS, first implemented in 1997, is also becoming more popular as a good way to determine molecular oligomerization in the membrane.⁶⁶ As long as the molecules of interest are sufficiently mobile in the membrane, FCS and FCCS can report on the dynamic processes in the membrane. FCCS has been used to look at dimerization or larger domain formation of different membrane proteins in the cell during cell activity.^{45,83} As such, it is an ideal method to detect organization of molecules on the

membrane, when the spatial scale of such organization is unknown. Detection of molecular interactions by Förster Resonance Energy Transfer (FRET) is good for determining very close interactions, such as dimerization of receptors, but it is likely to miss organization of molecules on membranes if the scale of such domains is beyond the Förster radius. Time-resolved photon arrival time data from PIE-FCCS allows both cross-correlation of differently labeled fluorescent species, but also possesses lifetime information of the fluorophore, which can be interpreted as FRET data. PIE-FCCS, then, can tell us about co-diffusional organization of molecules in the membrane and whether or not the fluorophores are close enough to undergo energy transfer.

3.5.2 Choosing the right fluorophores

Fluorescent proteins and organic dyes have very different photophysics, and even different fluorescent proteins can have different non-diffusion dependent processes (triplet states). It is important to characterize the behavior of the fluorescent proteins beforehand in order to determine if the protein is suitable for FCCS. FCCS depends on detecting the separate fluctuations of two separate fluorophores, so it is important to have two fluorophores that are sufficiently spectrally separated. GFP and Cherry are commonly used for colocalization. Even with the best optical filters, there is a small amount of bleed-thru of green photons into the Cherry detection channel, which can lead to false cross-correlation. Pulsed Interleaved Excitation temporally separates red and green signals, so that appropriate signals from each channel can be cross-correlated.

mCherry has a 40% chance of being excited to a triplet state which virtually makes it “dark” to the detectors.⁸⁴ Its measured brightness, on average, will appear to be less than GFP. This may lead to a decrease in detected cross-correlation. Other far-red bright fluorescent protein, such as mKATE2, were considered for FCCS experiments. However, the photophysical effects of the mKATE2 protein appear to be slower than that of mCherry, nor does it appear to be much brighter. Since triplet state blinking occurs on the microsecond timescale, and diffusion in the membrane occurs on the 10-100 millisecond timescale, it is possible to resolve these two processes by FCS. It is also important to have an empirical measurement of complete cross-correlation in order to determine the maximum amount of cross-correlation measurable between an FCCS pair.

Details on the optics and filters used for our experiments can be found in chapter 2.3.5.

3.5.3 Power Scan

Because FCS depends on the fluorescence fluctuations of a few diffusing species, the molecules must be sufficiently bright. The signal to noise ratio depends on the brightness of the molecule.⁷⁴ In order to determine the proper amount of excitation power, a power series for each fluorophore should be completed. GFP is excited by a 479 nm pulsed laser diode and mCherry is excited by a 568 nm CW Krypton-Argon gas laser, pulsed with an Electro-optic modulator (EOM). Repetition rate of the laser pulse is 10 MHz in our experiments, although 5 MHz should work as well. For both GFP and mCherry, an average power between 1-3 μ W is ideal for fluorescent protein excitation; in this power regime, the amplitude of the autocorrelation curve at $\tau = 100\mu$ s, $G(100\mu$ s), which is inversely related to the number of diffusing particles detected, remains constant and the emission intensity is linear with respect to

the excitation power. Below this power, background noise will dominate and the amplitude will look artificially depressed and the calculated number of particles will increase as power goes down. Above this power, saturation effects and photobleaching begin to affect the measurements.⁷³ (see figure 3.3) Since the dead time (See chapter 3.5.5) reduces the cross-correlation amplitude at increasing intensities, it is better, when using a TCSPC card to acquire data for PIE-FCCS, to tune to the lowest laser power above noise effects where the auto-correlation amplitude is constant with respect to power, generally around 1 μW for GFP and 1.5 μW for mCherry.

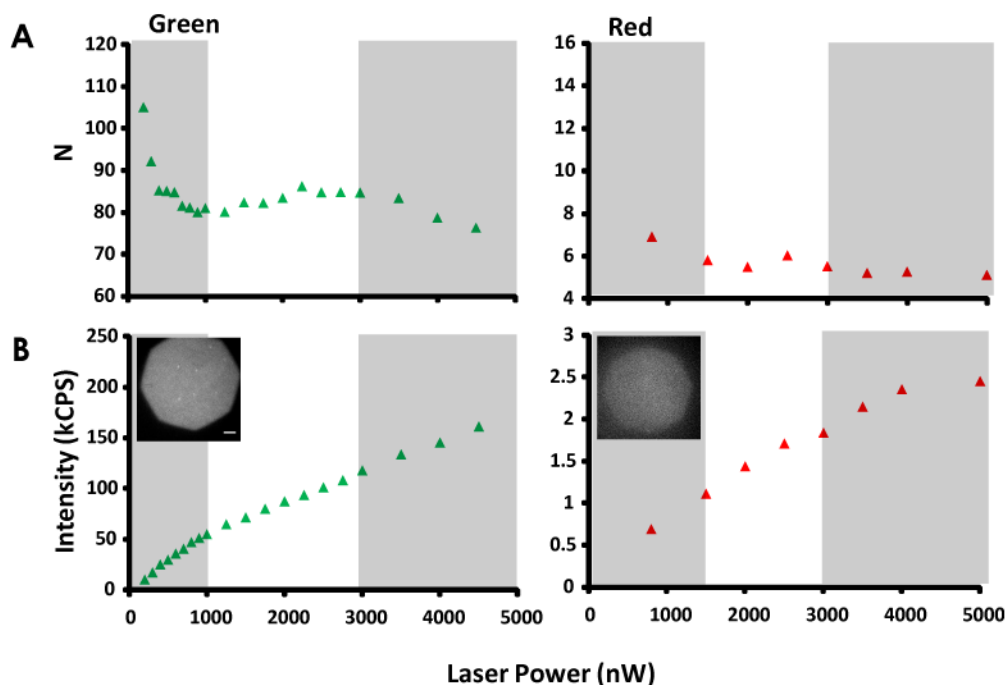


Figure 3.3. Power scan of GFP and Cherry. (A) Measure of N (inverse of the autocorrelation amplitude), number of diffusing species of GFP (left) and Cherry (right), at different excitation laser intensities, pulsing at 10 MHz. (B) Measure of increasing intensity with respect to laser excitation power. White window is the ideal power range, where N is constant and intensity rises linearly with excitation power. Inset images in (B) are epifluorescent images of GFP and Cherry, respectively. Scale bar is 10 μm .

3.5.4 Spot Size Measurement

An FCS autocorrelation trace can be fit to diffusional models to solve for the average residence time (τ_D) of a molecule diffusing through a laser spot. For our 2d geometry,

$$\tau_D = \frac{s^2}{4D} \quad (3.1)$$

where s is the radius of the spot area and D is the diffusion coefficient. Calibration with a fluorophore of a known diffusion constant can be used to determine the spot size, typically $\sim 0.1\text{-}0.15 \mu\text{m}^2$ (with beam profile ($2s$) of $\sim 500 \text{ nm}$ in diameter for the 568 nm laser). Generally, spot size does not vary significantly day to day, unless major re-alignment is performed. Once

the spot size is known, diffusion constants for His-tagged mCherry or mGFP tethered to supported lipid bilayers can be determined by fitting their diffusional autocorrelation curves to a 2d model mentioned in chapter 2.4.3 (Equation 2.4). Knowing this diffusion constant, it is possible to back out the spot size from the τ_D of the His-tagged fluorescent proteins each day, as long as the bilayer is consistently fluid and made fresh every day. Our empirically derived average diffusion constant of mCherry-His12 multivalently attached to a 2% Ni-NTA DGS bilayer is $\sim 1.26 \text{ } \mu\text{m}^2/\text{s}$, which is not unreasonable compared to other measured diffusion constants for lipids in model bilayers.^{52,85}

3.5.5 TCSPC advantage and disadvantage

Time resolution of photon detection, coupled with PIE, allows a multitude of uses from the same data. Concurrently with cross-talk free FCCS, fluorescence lifetime measurements can be used to determine the degree of energy transfer and a photon counting histogram can also be used to determine multimerization state of a fluorophore, based on the particle brightness.

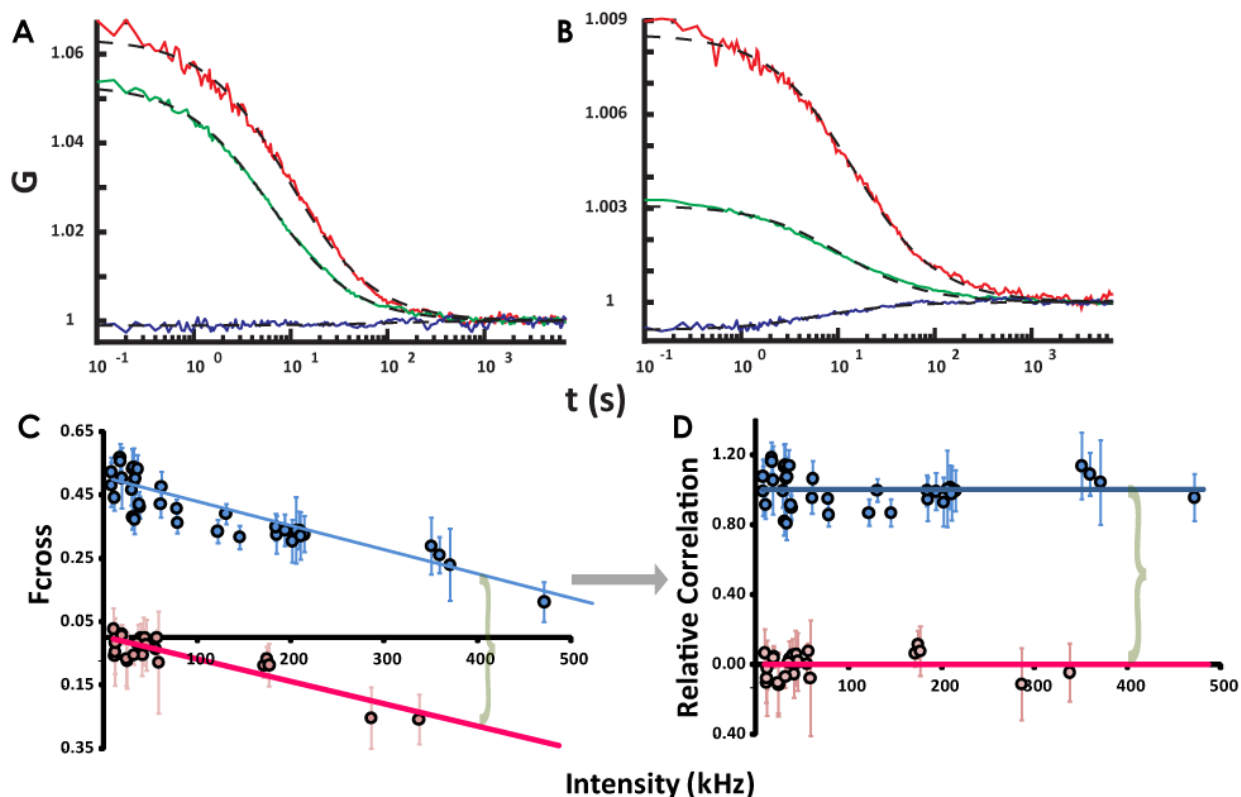


Figure 3.4. TCSPC card dead time decreases cross-correlation. (A and B) Auto- (red and green) and cross-correlation (blue) curves of mCherry-His12 and mGFP-His12 diffusing independently on a (A) 2 mol% Ni-NTA DGS bilayer and a (B) 6 mol% Ni-NTA-DGS bilayer. The increased Ni-NTA DGS concentration in (B) recruits more His-tagged protein to bind to the bilayer. Increased intensity leads to decreased cross-correlation, as a result of TCSPC card dead time. (C) Scatter plot of F_{cross} versus intensity of correlated mCherry-mGFP-His12 (\bullet) and uncorrelated mCherry-His12 and mGFP-His12 (\circ). Increased intensity comes from increased surface density of His-tagged fluorescent proteins. Decreasing cross-correlation with respect to intensity can be fit to a linear trend. F_{cross} values can be normalized to the interval between the correlated (blue line) and the uncorrelated (magenta line) states, designated by the gray bracket, and replotted on a normalized axis in (D).

The drawback to using a TCSPC card is that there is generally a longer “dead time” than there would be with conventional hardware correlators. This dead time causes an increasing percentage of time the TCSPC card is not detecting photons as the intensity of the sample increases. This means an increasingly negative effect on cross-correlation, with respect to intensity. This effect is detailed in chapter 2.4.2. We circumvent this effect by empirically mapping cross-correlation values to known physical states, as explained in chapter 3.4.1.

3.5.6 Spot selection in cells

When selecting areas to image for FCCS it is important to avoid parts of the cell where intracellular brightness obscures membrane fluorescence. Generally, areas on the periphery of the cell are optimal. Also, we focus on the bottom-side membrane adhered to the coverglass, since slow fluctuations of the top-side membrane will obscure lateral diffusional measurements. Diffusion of bright vesicles will also affect measurements, as will photobleaching effects of slow moving fractions. These effects can be seen in the intensity vs time traces and these traces should be discarded. Averaging several short traces (3-5 traces of 10-15s each) will result in smooth correlation curves.

Bibliography

1. Singer, S.J. & Nicolson, G.L. The fluid mosaic model of the structure of cell membranes. *Science (New York, N.Y.)* **175**, 720-31(1972).
2. Groves, J.T. & Kuriyan, J. Molecular mechanisms in signal transduction at the membrane. *Nature structural & molecular biology* **17**, 659-65(2010).
3. Karnovsky, M.J. et al. The concept of lipid domains in membranes. *The Journal of cell biology* **94**, 1-6(1982).
4. Brown, D. a & London, E. Functions of lipid rafts in biological membranes. *Annual review of cell and developmental biology* **14**, 111-36(1998).
5. Edidin, M. Membrane cholesterol, protein phosphorylation, and lipid rafts. *Science's STKE : signal transduction knowledge environment* **2001**, pe1(2001).
6. Kwik, J. et al. Membrane cholesterol, lateral mobility, and the phosphatidylinositol 4,5-bisphosphate-dependent organization of cell actin. *Proceedings of the National Academy of Sciences of the United States of America* **100**, 13964-9(2003).
7. Groves, J.T. Bending mechanics and molecular organization in biological membranes. *Annual review of physical chemistry* **58**, 697-717(2007).
8. Resh, M.D. Trafficking and signaling by fatty-acylated and prenylated proteins. *Nature chemical biology* **2**, 584-90(2006).
9. Brown, D.A. & Rose, J.K. Sorting of GPI-Anchored Proteins to Membrane Subdomains during Transport to the Apical Cell Surface. *Cell* **66**, 533-544(1992).
10. Zhang, W., Tribble, R.P. & Samelson, L.E. LAT palmitoylation: its essential role in membrane microdomain targeting and tyrosine phosphorylation during T cell activation. *Immunity* **9**, 239-46(1998).
11. Resh, M.D. Fatty acylation of proteins: new insights into membrane targeting of myristoylated and palmitoylated proteins. *Biochimica et biophysica acta* **1451**, 1-16(1999).
12. Simons, K. & Ikonen, E. Functional rafts in cell membranes. *Nature* **387**, 569-72(1997).
13. Zacharias, D.A. et al. Partitioning of lipid-modified monomeric GFPs into membrane microdomains of live cells. *Science* **296**, 913-6(2002).
14. Douglass, A.D. & Vale, R.D. Single-molecule microscopy reveals plasma membrane microdomains created by protein-protein networks that exclude or trap signaling molecules in T cells. *Cell* **121**, 937-50(2005).
15. Subramanian, K. et al. Palmitoylation determines the function of Vac8 at the yeast vacuole. *Journal of cell science* **119**, 2477-85(2006).
16. Orlean, P. & Menon, A.K. Thematic review series: lipid posttranslational modifications. GPI anchoring of protein in yeast and mammalian cells, or: how we learned to stop worrying and love glycopospholipids. *Journal of lipid research* **48**, 993-1011(2007).
17. McCabe, J.B. & Berthiaume, L.G. N-Terminal Protein Acylation Confers Localization to Cholesterol , Sphingolipid-enriched Membranes But Not to Lipid Rafts / Caveolae. *Molecular Biology of the Cell* **12**, 3601-3617(2001).
18. Bijlmakers, M.-J. & Marsh, M. The on-off story of protein palmitoylation. *Trends in cell biology* **13**, 32-42(2003).
19. Webb, Y., Hermida-Matsumoto, L. & Resh, M.D. Inhibition of protein palmitoylation, raft localization, and T cell signaling by 2-bromopalmitate and polyunsaturated fatty acids. *The Journal of biological chemistry* **275**, 261-70(2000).
20. Berthiaume, L.G. Insider information: how palmitoylation of Ras makes it a signaling double agent. *Science's STKE : signal transduction knowledge environment* **2002**, pe41(2002).
21. Klooster, J.P. ten & Hordijk, P.L. Targeting and localized signalling by small GTPases. *Biology of the cell / under the auspices of the European Cell Biology Organization* **99**, 1-12(2007).
22. Meer, G. van Cell biology. The different hues of lipid rafts. *Science (New York, N.Y.)* **296**, 855-7(2002).
23. Mukherjee, S. & Maxfield, F.R. Membrane domains. *Annual review of cell and developmental biology* **20**, 839-66(2004).
24. Henis, Y.I., Hancock, J.F. & Prior, I.A. Ras acylation, compartmentalization and signaling nanoclusters (Review). **26**, 80-92(2010).

25. Omerovic, J. & Prior, I.A. Compartmentalized signalling: Ras proteins and signalling nanoclusters. *The FEBS journal* **276**, 1817-25(2009).
26. Kabouridis, P.S., Magee, A.I. & Ley, S.C. S-acylation of LCK protein tyrosine kinase is essential for its signalling function in T lymphocytes. *The EMBO journal* **16**, 4983-98(1997).
27. Munro, S. Lipid Rafts Elusive or Illusive? *Cell* **115**, 377-388(2003).
28. Glebov, O.O. & Nichols, B.J. Lipid raft proteins have a random distribution during localized activation of the T-cell receptor. *Nature cell biology* **6**, 238-43(2004).
29. Nichols, B. Without a raft. *Nature* **436**, 638-9(2005).
30. Pike, L.J. Rafts defined: a report on the Keystone Symposium on Lipid Rafts and Cell Function. *Journal of lipid research* **47**, 1597-8(2006).
31. Pike, L.J. The challenge of lipid rafts. *Journal of lipid research* **50 Suppl**, S323-8(2009).
32. Hancock, J.F. Lipid rafts: contentious only from simplistic standpoints. *Nature reviews. Molecular cell biology* **7**, 456-62(2006).
33. Heerklotz, H. Triton promotes domain formation in lipid raft mixtures. *Biophysical journal* **83**, 2693-701(2002).
34. McConnell, H.M. & Vrljic, M. Liquid-liquid immiscibility in membranes. *Annual review of biophysics and biomolecular structure* **32**, 469-92(2003).
35. McConnell, H. Complexes in ternary cholesterol-phospholipid mixtures. *Biophysical journal* **88**, L23-5(2005).
36. Veatch, S.L. & Keller, S.L. Organization in Lipid Membranes Containing Cholesterol. *Physical Review Letters* **89**, 1-4(2002).
37. Veatch, S.L. & Keller, S.L. Separation of Liquid Phases in Giant Vesicles of Ternary Mixtures of Phospholipids and Cholesterol. *Biophysical Journal* **85**, 3074-3083(2003).
38. Baumgart, T., Hess, S.T. & Webb, W.W. Imaging coexisting fluid domains in biomembrane models coupling curvature and line tension. *Nature* **425**, 821-4(2003).
39. Veatch, S.L. & Keller, S.L.; A Closer Look at the Canonical "Raft Mixture" in Model Membrane Studies. *Biophysical Journal* **84**, 725-726(2003).
40. Kaiser, H.-J. et al. Order of lipid phases in model and plasma membranes. *Proceedings of the National Academy of Sciences of the United States of America* **106**, 16645-50(2009).
41. Baumgart, T. et al. Large-scale fluid/fluid phase separation of proteins and lipids in giant plasma membrane vesicles. *Proceedings of the National Academy of Sciences of the United States of America* **104**, 3165-70(2007).
42. Hammond, A.T. et al. Crosslinking a lipid raft component triggers liquid ordered-liquid disordered phase separation in model plasma membranes. *Proceedings of the National Academy of Sciences of the United States of America* **102**, 6320-5(2005).
43. Albertazzi, L. et al. Quantitative FRET analysis with the EGFP-mCherry fluorescent protein pair. *Photochemistry and photobiology* **85**, 287-97(2009).
44. Berney, C. & Danuser, G. FRET or no FRET: a quantitative comparison. *Biophysical journal* **84**, 3992-4010(2003).
45. Lillemeier, B.F. et al. TCR and Lat are expressed on separate protein islands on T cell membranes and concatenate during activation. *Nature immunology* **11**, 90-6(2010).
46. Owen, D.M. et al. PALM imaging and cluster analysis of protein heterogeneity at the cell surface. *Journal of biophotonics* **3**, 446-54(2010).
47. Kusumi, A. et al. Paradigm shift of the plasma membrane concept from the two-dimensional continuum fluid to the partitioned fluid: high-speed single-molecule tracking of membrane molecules. *Annual review of biophysics and biomolecular structure* **34**, 351-78(2005).
48. Kenworthy, A.K. et al. Dynamics of putative raft-associated proteins at the cell surface. *The Journal of cell biology* **165**, 735-46(2004).
49. Scherfeld D Fluorescence Correlation Spectroscopy relates rafts in model and native membranes. *Biophysical journal* **87**, 1034-1043(2004).
50. Lenne, P.-F. et al. Dynamic molecular confinement in the plasma membrane by microdomains and the cytoskeleton meshwork. *The EMBO journal* **25**, 3245-56(2006).
51. Vrljic, M., Nishimura, S.Y. & Moerner, W.E. Single-Molecule Tracking. *Methods in Molecular Biology, Vol. 398: Lipid Rafts* 193-219(2009).
52. Day, C. a & Kenworthy, A.K. Tracking microdomain dynamics in cell membranes. *Biochimica et biophysica acta* **1788**, 245-53(2009).

53. Quinn, P.J. A lipid matrix model of membrane raft structure. *Progress in lipid research* **49**, 390-406(2010).
54. Mayor, S. & Rao, M. Rafts: scale-dependent, active lipid organization at the cell surface. *Traffic* **5**, 231-40(2004).
55. Engelman, D.M. Membranes are more mosaic than fluid. *Nature* **438**, 578-80(2005).
56. Bhatnagar, R.S. & Gordon, J.I. Understanding covalent modifications of proteins by lipids: where cell biology and biophysics mingle. *Trends in cell biology* **7**, 14-20(1997).
57. Magee, T. & Seabra, M.C. Fatty acylation and prenylation of proteins: what's hot in fat. *Current opinion in cell biology* **17**, 190-6(2005).
58. Prior, I.A. et al. Direct visualization of Ras proteins in spatially distinct cell surface microdomains. *The Journal of cell biology* **160**, 165-70(2003).
59. Müller, B.K. et al. Pulsed interleaved excitation. *Biophysical journal* **89**, 3508-22(2005).
60. Levental, I. et al. Palmitoylation regulates raft affinity for the majority of integral raft proteins. *Proceedings of the National Academy of Sciences* **107**, 22050(2010).
61. Arni, S. et al. Association of GAP-43 with detergent-resistant membranes requires two palmitoylated cysteine residues. *The Journal of biological chemistry* **273**, 28478-85(1998).
62. Lichtenberg, D., Goñi, F.M. & Heerklotz, H. Detergent-resistant membranes should not be identified with membrane rafts. *Trends in biochemical sciences* **30**, 430-6(2005).
63. Veatch, S.L. & Keller, S.L. Seeing spots : Complex phase behavior in simple membranes. *Biochimica et biophysica acta* **1746**, 172 - 185(2005).
64. London, E. Insights into lipid raft structure and formation from experiments in model membranes. *Current Opinion in Structural Biology* **12**, 480-486(2002).
65. Johnson, S. a et al. Temperature-dependent phase behavior and protein partitioning in giant plasma membrane vesicles. *Biochimica et biophysica acta* **1798**, 1427-35(2010).
66. Schwille, P., Meyer-Almes, F.J. & Rigler, R. Dual-color fluorescence cross-correlation spectroscopy for multicomponent diffusional analysis in solution. *Biophysical journal* **72**, 1878-86(1997).
67. Lamb, D.C., Müller, B.K. & Bräuchle, C. Enhancing the sensitivity of fluorescence correlation spectroscopy by using time-correlated single photon counting. *Current pharmaceutical biotechnology* **6**, 405-14(2005).
68. Lin, W.-C. et al. Supported Membrane Formation, Characterization, Functionalization, and Patterning for Application in Biological Science and Technology. *Current Protocols in Chemical Biology* 235-269(2010).at <<http://dx.doi.org/10.1002/9780470559277.ch100131>>
69. Nye, J.A. & Groves, J.T. Kinetic control of histidine-tagged protein surface density on supported lipid bilayers. *Langmuir : the ACS journal of surfaces and colloids* **24**, 4145-9(2008).
70. Wohland, T., Rigler, R. & Vogel, H. The Standard Deviation in Fluorescence Correlation Spectroscopy. *Biophysical journal* **80**, 2987-2999(2001).
71. Legler, D.F. et al. Differential insertion of GPI-anchored GFPs into lipid rafts of live cells. *FASEB* **19**, 73-5(2005).
72. Janosi, L. & Gorfe, A.A. Segregation of negatively charged phospholipids by the polycationic and farnesylated membrane anchor of K-Ras. *Biophysical journal* **99**, 3666-74(2010).
73. Bacia, K. & Schwille, P. Practical guidelines for dual-color fluorescence cross-correlation spectroscopy. *Nature protocols* **2**, 2842-56(2007).
74. Lakowicz, J.R. *Principles of Fluorescence Spectroscopy*. 105(Springer: New York, 2006).
75. Albertazzi, L. et al. Quantitative FRET analysis with the EGFP-mCherry fluorescent protein pair. *Photochemistry and photobiology* **85**, 287-97(2009).
76. Ehrlich, L.I.R. et al. Dynamics of p56lck translocation to the T cell immunological synapse following agonist and antagonist stimulation. *Immunity* **17**, 809-22(2002).
77. Bunnell, S.C. T cell receptor ligation induces the formation of dynamically regulated signaling assemblies. *The Journal of Cell Biology* **158**, 1263-1275(2002).
78. Janosch, S. et al. Partitioning of Dual-Lipidated Peptides into Membrane Microdomains : Lipid Sorting vs Peptide Aggregation. *Biochemistry* 7496-7503(2004).
79. Edidin, M. The state of lipid rafts: from model membranes to cells. *Annual review of biophysics and biomolecular structure* **32**, 257-83(2003).
80. Melkonian, K. a et al. Role of lipid modifications in targeting proteins to detergent-resistant membrane rafts. Many raft proteins are acylated, while few are prenylated. *The Journal of biological chemistry* **274**, 3910-7(1999).

81. Silvius, J.R. CHAPTER 13 Lipidated Peptides as Tools for Understanding the Membrane Interactions of Lipid-Modified Proteins. *Current* **52**, (2002).
82. Rowat, A.C. et al. Farnesylated peptides in model membranes: a biophysical investigation. *European biophysics journal : EBJ* **33**, 300-9(2004).
83. Larson, D.R. et al. Temporally resolved interactions between antigen-stimulated IgE receptors and Lyn kinase on living cells. *The Journal of cell biology* **171**, 527-36(2005).
84. Hendrix, J. et al. Dark states in monomeric red fluorescent proteins studied by fluorescence correlation and single molecule spectroscopy. *Biophysical journal* **94**, 4103-13(2008).
85. Parthasarathy, R. & Groves, J.T. Protein patterns at lipid bilayer junctions. *Proceedings of the National Academy of Sciences of the United States of America* **101**, 12798-803(2004).

Appendix A

Primers and Gene Sequences:

Truncated anchor fluorescent fusion proteins in pN1 vector (restriction sites in bold):

LCK-NT-GFP

CCATGGGTTGTGTCTGCAGCTCAAACCCTGAAAAAAGAAGAAAAAGGGTGGCGG
TGGCCTCGAGATGGTGAGCAAGGGCGAGGAGCTGTTCACCGGGGTGGTGCCCATC
CTGGTTCGAGCTGGACGGCGACGTAAACGGCCACAAGTTCAGCGTGTCCGGCGAGG
GCGAGGGCGATGCCACcTACGGCAAGCTGACCCTGAAGTTCATCTGCACCACCGGC
AAGCTGCCCCGTGCCCTGGCCCACCCTCGTGACCACCCTGACCTACGGCGTGCAGTG
CTTCAGCCGCTACCCCGACCATGAAGCAGCAGACTTCTTCAAGTCCGCCATGC
CCGAAGGCTACGTCCAGGAGCGCACCATCTTCTTCAAGGACGACGGCAACTACAAG
ACCCGCGCCGAGGTGAAGTTCGAGGGCGACACCCTGGTGAACCGCATCGAGCTGA
AGGGCATCGACTTCAAGGAGGACGGCAACATCCTGGGGCACAAGCTGGAGTACAA
CTACAACAGCCACAACGTCTATATCATGGCCGACAAGCAGAAGAACGGCATCAAG
GTGAACTTCAAGATCCGCCACAACATCGAGGACGGCAGCGTGCAGCTCGCCGACCA
CTACCAGCAGAACACCCCCATCGGCGACGGCCCCGTGCTGCTGCCCCGACAACCACT
ACCTGAGCACCCAGTCCGCCCTGAGCAAAGACCCCAACGAGAAGCGCGATCACAT
GGTCCTGCTGGAGTTCGTGACCGCCGCCGGGATCACTCTCGGCATGGACGAGCTGT
ACAAGTAAGCGGCCGC

LCK-NT-mCherry

CCATGGGTTGTGTCTGCAGCTCAAACCCTGAAAAAAGAAGAAAAAGGGTGGCGG
TGGCCTCGAGATGGTGAGCAAGGGCGAGGAGGACAACATGGCCATCATCAAGGAG
TTCATGCGGTTCAAGGTGCACATGGAGGGCAGCGTGAACGGCCACGAGTTCGAGAT
CGAGGGCGAGGGCGAGGGCAGACCcTACGAGGGCACCCAGACCGCCAAGCTGAAG
GTGACCAAGGGCGGCCCTCTGCCCTTCGCCTGGGACATCCTGAGCCCCCAGTTCAT
GTACGGCAGCAAGGCCTACGTGAAGCACCTGCCGACATCCCCGACTACCTGAAGC
TGAGCTTCCCCGAGGGCTTCAAGTGGGAGAGAGTGATGAACTTCGAGGACGGCGG
CGTGGTGACCGTGACCCAGGACTCCTCTCTGCAGGACGGCGAGTTCATCTACAAGG
TGAAGCTGAGGGGCACCAACTTCCCTAGCGACGGCCCAGTGATGCAGAAGAAGAC
AATGGGCTGGGAGGCCAGCTCCGAGAGAATGTACCCCGAGGACGGCGCCCTGAAG
GGCGAGATCAAGCAGAGACTGAAGCTGAAGGACGGCGGCCACTACGACGCCGAGG
TGAAGACCACCTACAAGGCCAAGAAGCCCGTGCAGCTGCCCGGCGCCTACAACGT
GAACATCAAGCTGGACATCACCTCTCACAACGAGGACTACCCATCGTGGAGCAGT
ACGAGCGCGCCGAGGGCAGGCACAGCACAGGCGGCATGGACGAGCTGTACAAGTA
AGCGGCCGC

GFP-RhoA-CT

**CCATGGTGAGCAAGGGCGAGGAGCTGTTACCGGGGTGGTGCCCATCCTGGTCGA
GCTGGACGGCGACGTAAACGGCCACAAGTTCAGCGTGTCCGGCGAGGGCGAGGGC
GATGCCACCTACGGCAAGCTGACCCTGAAGTTCATCTGCACCACCGGCAAGCTGCC
CGTGCCCTGGCCCACCCTCGTGACCACCCTGACCTACGGCGTGCAGTGCTTCAGCC
GCTACCCCGACCACATGAAGCAGCACGACTTCTTCAAGTCCGCCATGCCCGAAGGC
TACGTCCAGGAGCGCACCATCTTCTTCAAGGACGACGGCAACTACAAGACCCGCGC
CGAGGTGAAGTTCGAGGGCGACACCCTGGTGAACCGCATCGAGCTGAAGGGCATC
GACTTCAAGGAGGACGGCAACATCCTGGGGCACAAGCTGGAGTACA ACTACAACA
GCCACAACGTCTATATCATGGCCGACAAGCAGAAGAACGGCATCAAGGTGAACTTC
AAGATCCGCCACAACATCGAGGACGGCAGCGTGCAGCTCGCCGACCACTACCAGC
AGAACACCCCATCGGGCGACGGCCCCGTGCTGCTGCCCGACAACCACTACCTGAGC
ACCCAGTCCGCCCTGAGCAAAGACCCCAACGAGAAGCGCGATCACATGGTCCTGCT
GGAGTTCGTGACCGCCGCCGGGATCACTCTCGGCATGGACGAGCTGTACAAGTCCG
GACTCAGATCTGGTGCTAGACGTGGGAAGAAAAAGTCTGGGTGCCTCATCTTGTGA
GCGGCCGC**

mCherry-RhoA-CT

**CCATGGTGAGCAAGGGCGAGGAGGACAACATGGCCATCATCAAGGAGTTCATGCG
GTTCAAGGTGCACATGGAGGGCAGCGTGAACGGCCACGAGTTCGAGATCGAGGGC
GAGGGCGAGGGCAGACCCTACGAGGGCACCCAGACCGCCAAGCTGAAGGTGACCA
AGGGCGGCCCTCTGCCCTTCGCCTGGGACATCCTGAGCCCCAGTTCATGTACGGC
AGCAAGGCCTACGTGAAGCACCCCTGCCGACATCCCCGACTACCTGAAGCTGAGCTT
CCCCGAGGGGCTTCAAGTGGGAGAGAGTGATGAACTTCGAGGACGGCGGCGTGGTG
ACCGTGACCCAGGACTCCTCTCTGCAGGACGGCGAGTTCATCTACAAGGTGAAGCT
GAGGGGCACCAACTTCCCTAGCGACGGCCCCAGTGATGCAGAAGAAGACAATGGGC
TGGGAGGCCAGCTCCGAGAGAATGTACCCCGAGGACGGCGCCCTGAAGGGCGAGA
TCAAGCAGAGACTGAAGCTGAAGGACGGCGGCCACTACGACCGCGAGGTGAAGAC
CACCTACAAGGCCAAGAAGCCCGTGCAGCTGCCCGGCGCCTACAACGTGAACATCA
AGCTGGACATCACCTCTCACAACGAGGACTACACCATCGTGGAGCAGTACGAGCGC
GCCGAGGGCAGGCACAGCACAGGCGGCATGGACGAGCTGTACAAGTCCGGACTCA
GATCTGGTGCTAGACGTGGGAAGAAAAAGTCTGGGTGCCTCATCTTGTGAGCGGC
CGC**

GFP-kRas-CT

**CCATGGTGAGCAAGGGCGAGGAGCTGTTACCGGGGTGGTGCCCATCCTGGTCGA
GCTGGACGGCGACGTAAACGGCCACAAGTTCAGCGTGTCCGGCGAGGGCGAGGGC
GATGCCACCTACGGCAAGCTGACCCTGAAGTTCATCTGCACCACCGGCAAGCTGCC
CGTGCCCTGGCCCACCCTCGTGACCACCCTGACCTACGGCGTGCAGTGCTTCAGCC
GCTACCCCGACCACATGAAGCAGCACGACTTCTTCAAGTCCGCCATGCCCGAAGGC
TACGTCCAGGAGCGCACCATCTTCTTCAAGGACGACGGCAACTACAAGACCCGCGC
CGAGGTGAAGTTCGAGGGCGACACCCTGGTGAACCGCATCGAGCTGAAGGGCATC**

GACTTCAAGGAGGACGGCAACATCCTGGGGCACAAGCTGGAGTACAACACTACAACA
GCCACAACGTCTATATCATGGCCGACAAGCAGAAGAACGGCATCAAGGTGAACTTC
AAGATCCGCCACAACATCGAGGACGGCAGCGTGCAGCTCGCCGACCACTACCAGC
AGAACACCCCCATCGGCGACGGCCCCGTGCTGCTGCCCGACAACCACTACCTGAGC
ACCCAGTCCAAGCTGAGCAAAGACCCCAACGAGAAGCGCGATCACATGGTCCTGCT
GGAGTTCGTGACCGCCGCCGGGATCACTCTCGGCATGGACGAGCTGTACAAGAAA
AAAAGAAAAAATCCAAGACCAAGTGCGTGATCATGTAATGCGGCCGC

mCherry-kRas-CT

CCATGGTGAGCAAGGGCGAGGAGGATAACATGGCCATCATCAAGGAGTTCATGCG
CTTCAAGGTGCACATGGAGGGCTCCGTGAACGGCCACGAGTTCGAGATCGAGGGC
GAGGGCGAGGGCCGCCCTACGAGGGCACCCAGACCGCCAAGCTGAAGGTGACCA
AGGGTGGCCCCCTGCCCTTCGCCTGGGACATCCTGTCCCCTCAGTTCATGTACGGCT
CCAAGGCCTACGTGAAGCACCCCGCCGACATCCCCGACTACTTGAAGCTGTCCTTC
CCCGAGGGCTTCAAGTGGGAGCGCGTGATGAACTTCGAGGACGGCGGCGTGTTGA
CCGTGACCCAGGACTCCTCCCTGCAGGACGGCGAGTTCATCTACAAGGTGAAGCTG
CGCGGCACCAACTTCCCCTCCGACGGCCCCGTAATGCAGAAGAAGACCATGGGCTG
GGAGGCCTCCTCCGAGCGGATGTACCCCGAGGACGGCGCCCTGAAGGGCGAGATC
AAGCAGAGGCTGAAGCTGAAGGACGGCGGCCACTACGACGCTGAGGTCAAGACCA
CCTACAAGGCCAAGAAGCCCCTGCAGCTGCCCGGCGCCTACAACGTCAACATCAAG
TTGGACATCACCTCCCACAACGAGGACTACACCATCGTGGAACAGTACGAACGCGC
CGAGGGCCGCCACTCCACCGGCGGCATGGACGAGCTGTACAAGAAAAAAGAAA
AAATCCAAGACCAAGTGCGTGATCATGTAATGCGGCCGC

mCherry-mGFP-kRas-CT

CCATGGTGAGCAAGGGCGAGGAGGATAACATGGCCATCATCAAGGAGTTCATGCG
CTTCAAGGTGCACATGGAGGGCTCCGTGAACGGCCACGAGTTCGAGATCGAGGGC
GAGGGCGAGGGCCGCCCTACGAGGGCACCCAGACCGCCAAGCTGAAGGTGACCA
AGGGTGGCCCCCTGCCCTTCGCCTGGGACATCCTGTCCCCTCAGTTCATGTACGGCT
CCAAGGCCTACGTGAAGCACCCCGCCGACATCCCCGACTACTTGAAGCTGTCCTTC
CCCGAGGGCTTCAAGTGGGAGCGCGTGATGAACTTCGAGGACGGCGGCGTGTTGA
CCGTGACCCAGGACTCCTCCCTGCAGGACGGCGAGTTCATCTACAAGGTGAAGCTG
CGCGGCACCAACTTCCCCTCCGACGGCCCCGTAATGCAGAAGAAGACCATGGGCTG
GGAGGCCTCCTCCGAGCGGATGTACCCCGAGGACGGCGCCCTGAAGGGCGAGATC
AAGCAGAGGCTGAAGCTGAAGGACGGCGGCCACTACGACGCTGAGGTCAAGACCA
CCTACAAGGCCAAGAAGCCCCTGCAGCTGCCCGGCGCCTACAACGTCAACATCAAG
TTGGACATCACCTCCCACAACGAGGACTACACCATCGTGGAACAGTACGAACGCGC
CGAGGGCCGCCACTCCACCGGCGGCATGGACGAGCTGTACAAGCGGG**ATCCACCG**
GTCGCCACCATGGTGAGCAAGGGCGAGGAGCTGTTACCGGGGTGGTGCCCATCC
TGGTCGAGCTGGACGGCGACGTAAACGGCCACAAGTTCAGCGTGTCCGGCGAGGG
CGAGGGCGATGCCACNTACGGCAAGCTGACCCTGAAGTTCATCTGCACCACCGGCA
AGCTGCCCCGTGCCCTGGCCCACCTCGTGACCACCTGACNTACGGCGTGCAAGTGC

TTCAGCCGCTACCCCGACCATGAAGCAGCACGACTTCTTCAAGTCCGCCATGCC
CGAAGGCTACGTCCAGGAGCGCACCATCTTCTTCAAGGACGACGGCAACTACAAGA
CCCGCGCCGAGGTGAAGTTCGAGGGCGACACCCTGGTGAACCGCATCGAGCTGAA
GGGCATCGACTTCAAGGAGGACGGCAACATCCTGGGGCACAAGCTGGAGTACAAC
TACAACAGCCACAACGTCTATATCATGGCCGACAAGCAGAAGAACGGCATCAAGG
TGAACCTCAAGATCCGCCACAACATCGAGGACGGCAGCGTGCAGCTCGCCGACCAC
TACCAGCAGAACACCCCATCGGCGACGGCCCCGTGCTGCTGCCCGACAACCACTA
CCTGAGCACCCAGTCCAAGCTGAGCAAAGACCCCAACGAGAAGCGCNATCACATG
GTCCTGCTGGAGTTCGTGACCGCCGCCGGGNTCACTCTCGGCATGGACGAGCTGTA
CAAGAAAAAAGAAAAAATCCAAGACCAAGTGCGTGATCATGTAAT**GCGGCCG**
C

His-tagged fluorescent proteins in pET28b(+) vector:

mGFP-His12

CCATGGGCAGCAGCATGGTGAGCAAGGGCGAGGAGCTGTTACCGGGGTGGTGCC
CATCCTGGTCGAGCTGGACGGCGACGTAAACGGCCACAAGTTCAGCGTGTCCGGCG
AGGGCGAGGGCGATGCCACCTACGGCAAGCTGACCCTGAAGTTCATCTGCACCACC
GGCAAGCTGCCCGTGCCCTGGCCCACCCTCGTGACCACCCTGACCTACGGCGTGCA
GTGCTTCAGCCGCTACCCCGACCATGAAGCAGCACGACTTCTTCAAGTCCGCCA
TGCCCGAAGGCTACGTCCAGGAGCGCACCATCTTCTTCAAGGACGACGGCAACTAC
AAGACCCGCGCCGAGGTGAAGTTCGAGGGCGACACCCTGGTGAACCGCATCGAGC
TGAAGGGCATCGACTTCAAGGAGGACGGCAACATCCTGGGGCACAAGCTGGAGTA
CAACTACAACAGCCACAACGTCTATATCATGGCCGACAAGCAGAAGAACGGCATC
AAGGTGAACTTCAAGATCCGCCACAACATCGAGGACGGCAGCGTGCAGCTCGCCG
ACCACTACCAGCAGAACACCCCATCGGCGACGGCCCCGTGCTGCTGCCCGACAAC
CACTACCTGAGCACCCAGTCCAAGCTGAGCAAAGACACCAACGAGAAGCGCGATC
ACATGGTCCTGCTGGAGTTCGTGACCGCCGCCGGGATCACTCTCGGCATGGACGAG
CTGTACAAGA**AAGCTT**CATCATCATCATCATCATCATCATCATCATCATTA**ACTC**
GAG

mCherry-His12

CCATGGGCAGCAGCATGGTGAGCAAGGGCGAGGAGGACAACATGGCCATCATCAA
GGAGTTCATGCGGTTCAAGGTGCACATGGAGGGCAGCGTGAACGGCCACGAGTTC
GAGATCGAGGGCGAGGGCGAGGGCAGACCCTACGAGGGCACCCAGACCGCCAAGC
TGAAGGTGACCAAGGGCGGCCCTCTGCCCTTCGCCTGGGACATCCTGAGCCCCAG
TTCATGTACGGCAGCAAGGCCTACGTGAAGCACCCCTGCCGACATCCCCGACTACCT
GAAGCTGAGCTTCCCCGAGGGCTTCAAGTGGGAGAGAGTGATGAACTTCGAGGAC
GGCGGCGTGGTGACCGTGACCCAGGACTCCTCTCTGCAGGACGGCGAGTTCATCTA
CAAGGTGAAGCTGAGGGGCACCAACTTCCCTAGCGACGGCCCAGTGATGCAGAAG
AAGACAATGGGCTGGGAGGCCAGCTCCGAGAGAATGTACCCCGAGGACGGCGCCC
TGAAGGGCGAGATCAAGCAGAGACTGAAGCTGAAGGACGGCGGCCACTACGACGC

CGAGGTGAAGACCACCTACAAGGCCAAGAAGCCCGTGCAGCTGCCCGGCGCCTAC
AACGTGAACATCAAGCTGGACATCACCTCTCACAACGAGGACTACACCATCGTGGA
GCAGTACGAGCGCGCCGAGGGCAGGCACAGCACAGGCGGCATGGACGAGCTGTAC
AAGAAGCTTCATCATCATCATCATCATCATCATCATCATCATCATTA**ACTCGAG**

mCherry-mGFP-His12

CCATGGGCAGCAGCATGGTGAGCAAGGGCGAGGAGGACAACATGGCCATCATCAA
GGAGTTCATGCGGTTCAAGGTGCACATGGAGGGCAGCGTGAACGGCCACGAGTTC
GAGATCGAGGGCGAGGGCGAGGGCAGACCCTACGAGGGCACCCAGACCGCCAAGC
TGAAGGTGACCAAGGGCGGCCCTCTGCCCTTCGCCTGGGACATCCTGAGCCCCAG
TTCATGTACGGCAGCAAGGCCTACGTGAAGCACCCCTGCCGACATCCCCGACTACCT
GAAGCTGAGCTTCCCCGAGGGCTTCAAGTGGGAGAGAGTGATGAACTTCGAGGAC
GGCGGCGTGGTGACCGTGACCCAGGACTCCTCTCTGCAGGACGGCGAGTTCATCTA
CAAGGTGAAGCTGAGGGGCACCAACTTCCCTAGCGACGGCCCAGTGATGCAGAAG
AAGACAATGGGCTGGGAGGCCAGCTCCGAGAGAATGTACCCCGAGGACGGCGCCC
TGAAGGGCGAGATCAAGCAGAGACTGAAGCTGAAGGACGGCGGCCACTACGACGC
CGAGGTGAAGACCACCTACAAGGCCAAGAAGCCCGTGCAGCTGCCCGGCGCCTAC
AACGTGAACATCAAGCTGGACATCACCTCTCACAACGAGGACTACACCATCGTGGA
GCAGTACGAGCGCGCCGAGGGCAGGCACAGCACAGGCGGCATGGACGAGCTGTAC
AAGGGATCCATGGTGAGCAAGGGCGAGGAGCTGTTACCCGGGGTGGTGCCCATCC
TGGTCGAGCTGGACGGCGACGTAAACGGCCACAAGTTCAGCGTGTCCGGCGAGGG
CGAGGGCGATGCCACCTACGGCAAGCTGACCCTGAAGTTCATCTGCACCACCGGCA
AGCTGCCCCTGCCCTGGCCACCCTCGTGACCACCCTGACCTACGGCGTGCAGTGC
TTCAGCCGCTACCCCGACCACATGAAGCAGCACGACTTCTTCAAGTCCGCCATGCC
CGAAGGCTACGTCCAGGAGCGCACCATCTTCTTCAAGGACGACGGCAACTACAAGA
CCCGCGCCGAGGTGAAGTTCGAGGGCGACACCCTGGTGAACCGCATCGAGCTGAA
GGGCATCGACTTCAAGGAGGACGGCAACATCCTGGGGCACAAGCTGGAGTACAAC
TACAACAGCCACAACGTCTATATCATGGCCGACAAGCAGAAGAACGGCATCAAGG
TGAATTCAAGATCCGCCACAACATCGAGGACGGCAGCGTGCAGCTCGCCGACCAC
TACCAGCAGAACACCCCATCGGCGACGGCCCCGTGCTGCTGCCCGACAACCACTA
CCTGAGCACCCAGTCCAAGCTGAGCAAAGACaCCAACGAGAAGCGCGATCACATGG
TCCTGCTGGAGTTCGTGACCGCCGCCGGGATCACTCTCGGCATGGACGAGCTGTAC
AAGAAGCTTCATCATCATCATCATCATCATCATCATCATCATCATTA**ACTCGAG**

Primers

His12 Adapter

GGCCAAGCTTCATCATCATCATCATCATCATCATCATCATCATCATTA**ACTCGAGG**
GCC

For cloning FP into pET28b(+)-His12

P1: CCGGCCATGGGCAGCAGCATGGTGAGCAAGGGCGAGGAG

P2 (RC): ggcgcgAAGCTTCTTGTACAGCTCGTCCATGCCG

For cloning FP1 and FP2 fusion

P3 (RC): GGCCGGATCCCTTGTACAGCTCGTCCATGCCG

P4: gccggcGGATCCATGGTGAGCAAGGGGCGAGGAG

For cloning LCK-NT-FP into PN1 (AgeI/NotI)

P5: GGCCGGCCACCGGTCGCCACCATGGGTTGTGTCTGCAGCTCAAACC

P6: GGCCGGCCGCGGCCGCTTACTTGTACAGCTCGTCCATGCCG

For cloning FP-RhoA-CT into PN1 (NcoI/NotI)

P7: GGCCGCCCATGGTGAGCAAGGGGCGAGGAG

P8: GGCCGCGCGGCCGCTCACAAGATGAGGCACCCAGAC